
Supplementary Information

Photochromic dye-sensitized solar cells with light-driven adjustable optical transmission and power conversion efficiency

Quentin Huauilmé,^a Valid M. Mwalukuku,^a Damien Joly,^a Johan Liotier,^a
Yann Kervella,^a Pascale Maldivi,^a Stéphanie Narbey,^b Frédéric Oswald,^b
Antonio J. Riquelme,^c Juan Antonio Anta,^c Renaud Demadrille^{a*}

a. CEA-Univ. Grenoble Alpes-CNRS, IRIG, SyMMES, 38000 Grenoble, France.

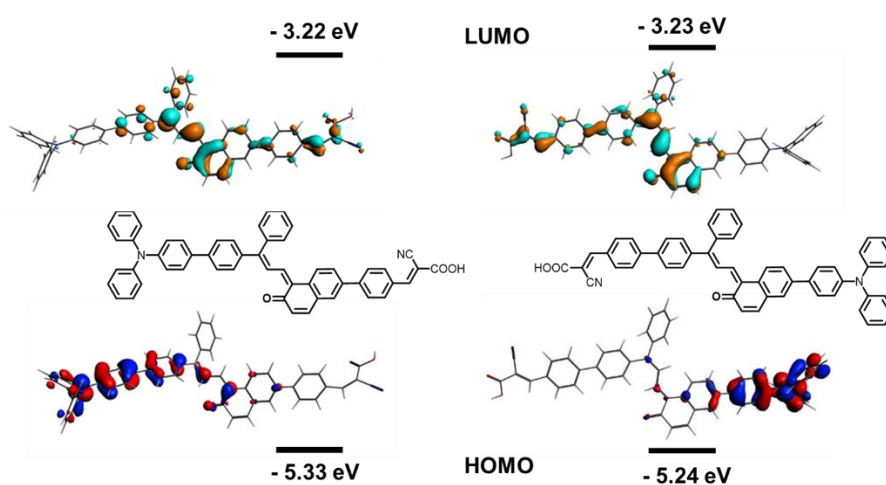
b. Solaronix SA, Rue de l'Ouriette 129, 1170 Aubonne, Switzerland

c. Área de Química Física, Departamento de Sistemas Físicos, Químicos y Naturales,
Universidad Pablo de Olavide, Sevilla, Spain

Supplementary Note 1

Photochromic dyes being non-symmetric, it is crucial to carefully choose the D and A functional groups positions to control the spatial localisation of the frontier orbitals as well as their energy level positions. These parameters were obtained through DFT calculations and modelling and helped us identify the most favourable orientation of the photochromic unit connection within the dye's structure. Indeed, three parts distinguish these photochromic systems: the diphenyl unit, the pyran unit, and the naphthalene unit. Only the diphenyl and naphthalene units can be functionalized, whereas any functionalization of the pyran cycle would cause the molecule to lose the photochromic

behaviour. The effects of two types of substitution were investigated, either the connection of a triphenylamine electron-donating unit on the diphenyl part or the connection of a phenyl-cyanoacrylic acid unit as both an electron-withdrawing unit and anchoring function on the naphthalene unit, or the other way around. **Supplementary Figure 1** shows two types of substitution for the open form of **NPL**. Our modelling show that energy levels of the frontiers orbitals are well positioned to allow photo-injection of electrons into the oxide and to allow regeneration of the oxidized species by the iodide-triiodide redox pair.



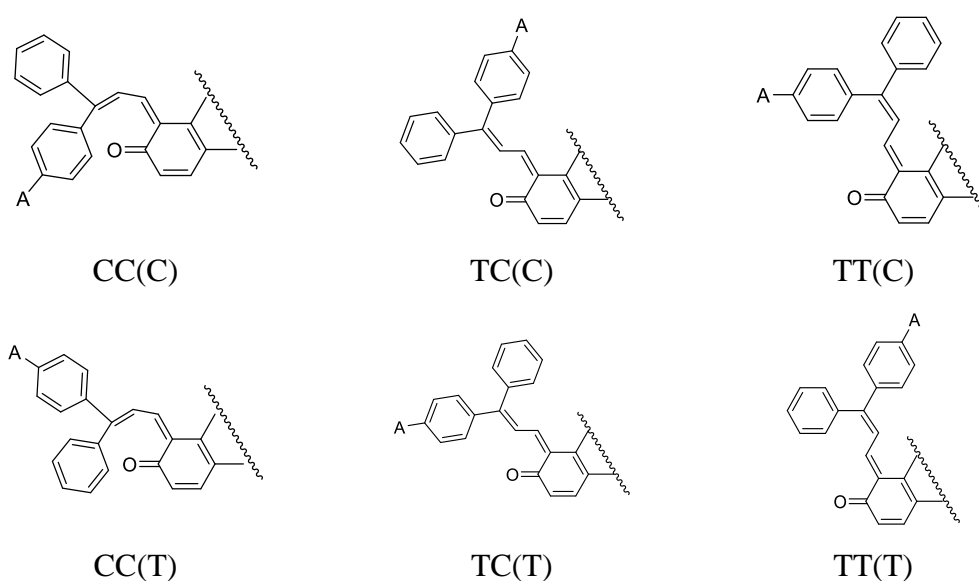
Supplementary Figure 1: HOMO-LUMO energy levels with respect to vacuum level and orbitals distribution according to the direction of functionalization for **NPL** photochromic compound. Calculation Optimisation PBE/TZ2P followed by SP B3LYP/TZ2P.

Interestingly, we notice that the dyes can theoretically behave as photosensitizers either in their closed or opened form, the open form being supposed to be more effective because it absorbs in the visible range. The substitution direction has a slight impact on the HOMO energy level with a variation of less than 0.1eV but it influences more significantly the position of the LUMO level. However, these levels remain compatible with our solar device configuration. They match well with those of the conduction band of the oxide (at ≈ -4.1 eV) and of the potential of the I^-/I_3^- redox couple used in the electrolyte (at ≈ -4.95 eV). The ΔE_{inj} higher than 0.6 eV and ΔE_{reg} higher than 0.3 eV are large enough to ensure a good injection of the photo-excited electrons in the oxide and the regeneration of the photo-oxidized dye molecules by the redox mediator.⁴⁹

As far as the orbital spatial distributions are concerned, when the electron-attractive unit is introduced on the naphthalene part, the electronic delocalization of the LUMO occurs

on almost the whole molecule, which is not favourable for effective photo-injection of electrons into the metal oxide. In that case, the photo-excited electron can thus be located very far from the oxide surface. On the contrary, the introduction of the anchoring function on the diphenyl part perfectly relocates the LUMO and leads to a better spatial separation of the frontier orbitals.

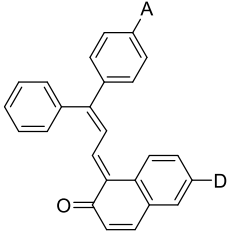
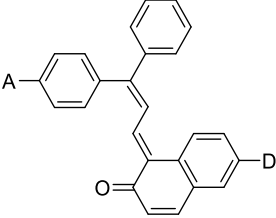
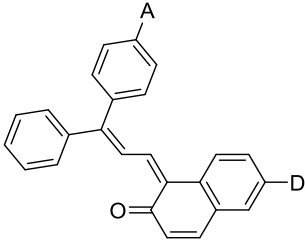
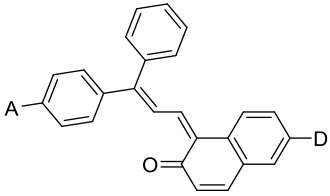
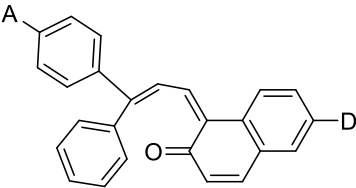
In order to simplify the naming, the D and A symbols will represent the triphenylamine electron-donor function and the phenyl-cyanoacrylic acid electron-acceptor group respectively.



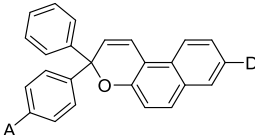
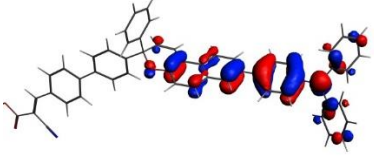
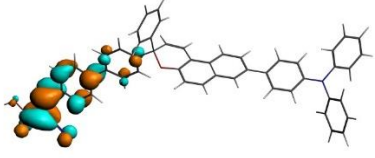
Supplementary Figure 2. Various possible conformations of the OF of substituted naphthopyran with their naming. The (T) or (C) notation refers to the position of the A acceptor group.

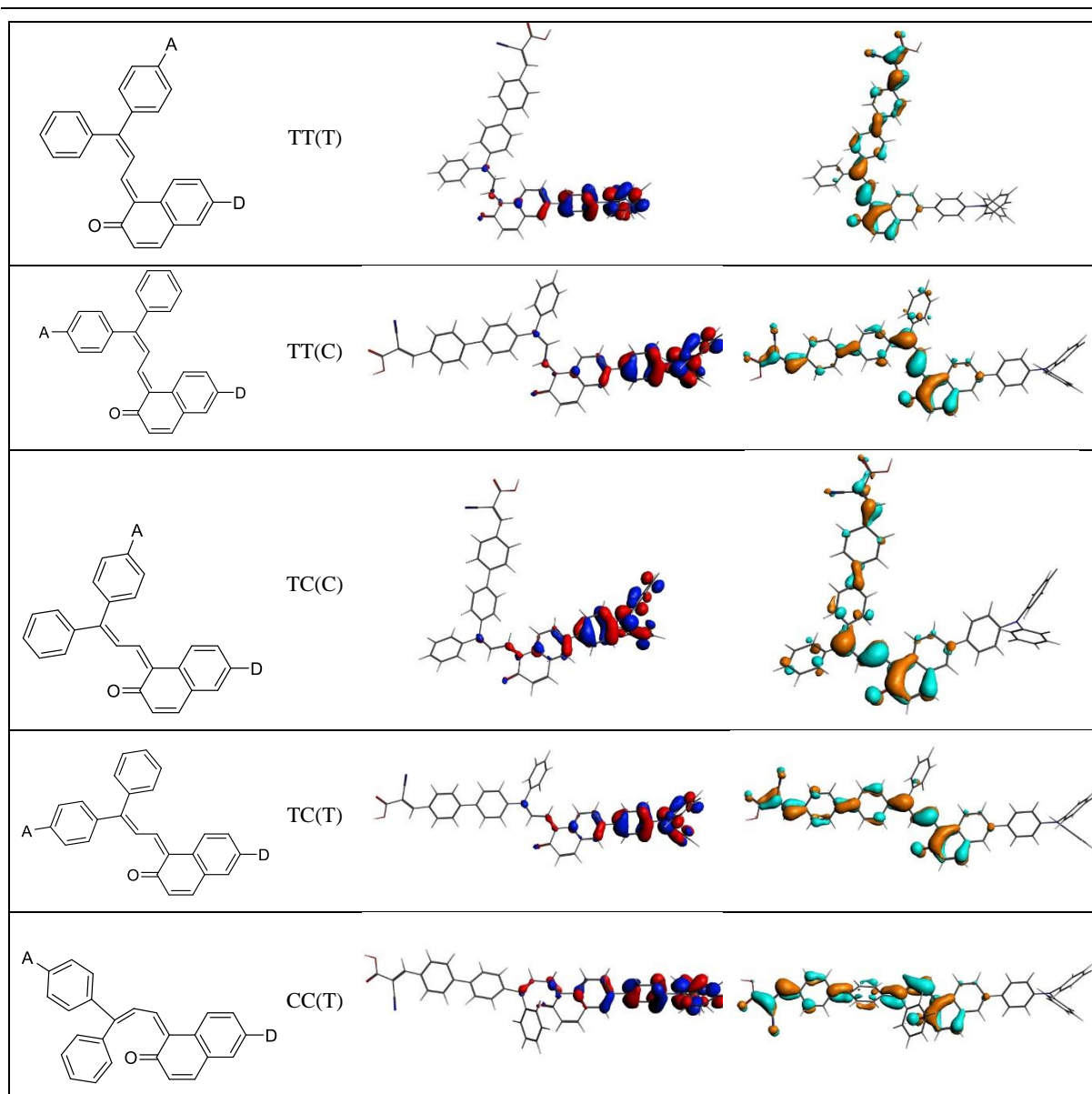
Supplementary Table 1. Relative energies ΔE_{SP} (kcal/mol) calculated at the B3LYPD3/TZ2P/COSMO level, eigenvalues of HOMO and LUMO, energy gap (eV) for the CF and OF geometries of NPL.

	Form	ΔE_{SP}	HOMO	LUMO	gap
	CF	0.0	-5.14	-2.93	2.21

	TT(T)	-0.71	-5.26	-3.22	2.04
	TT(C)	0.14	-5.25	-3.16	2.09
	CT(C)	-0.38	-5.22	-3.17	2.05
	CT(T)	-3.05	-5.24	-3.23	2.01
	CC(T)	6.59	-5.23	-3.08	2.15

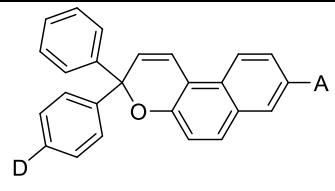
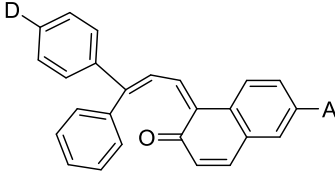
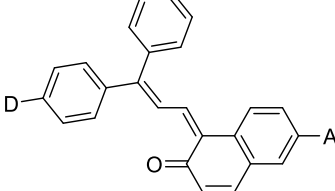
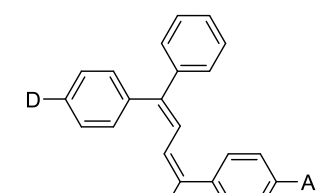
Supplementary Table 2. HOMO and LUMO localization for the CF and OF geometries of **NPL**, from the B3LYP single-points.

Form	HOMO	LUMO
 CF		



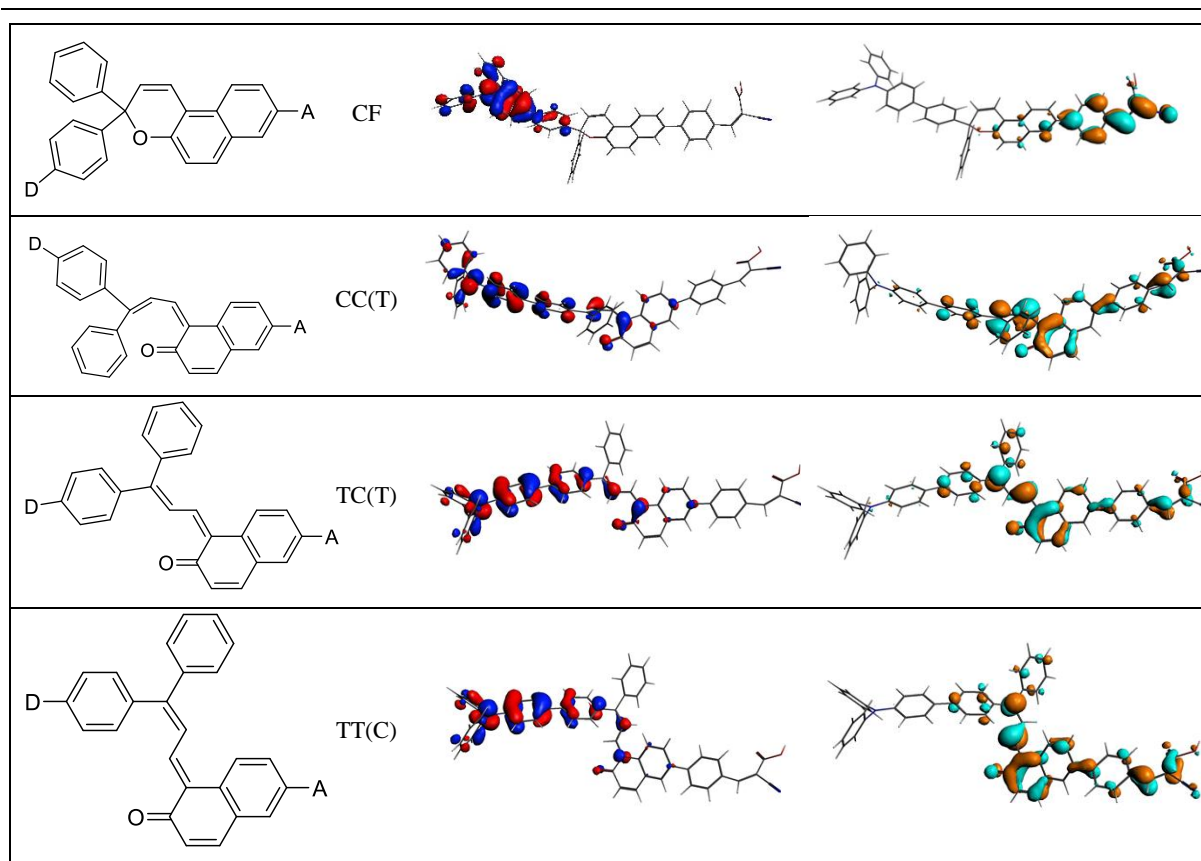
Supplementary Table 3. Relative energies ΔE_{sp} (kcal/mol) calculated at the B3LYPD3/TZ2P/COSMO level, eigenvalues of HOMO and LUMO, energy gap (eV) for the CF and OF geometries of **NPL** « exchanged ».

Form	ΔE_{sp}	HOMO	LUMO	gap
------	-----------------	------	------	-----

	CF	0.0	-5.30	-2.62	2.68
	CC(T)	19.9	-5.29	-3.25	2.04
	TC(T)	12.6	-5.31	-3.26	2.05
	TT(C)	12.6	-5.33	-3.22	2.11

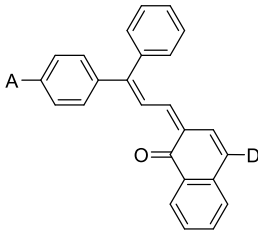
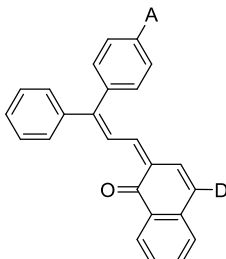
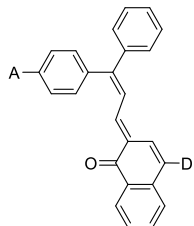
Supplementary Table 4. HOMO and LUMO localization for the CF and OF geometries of NPL « exchanged », from the B3LYP single-points.

Form	HOMO	LUMO
------	------	------

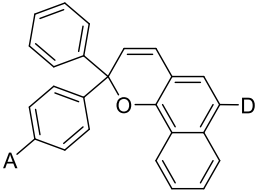
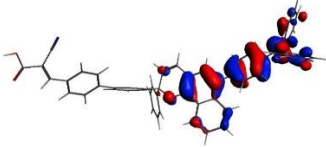
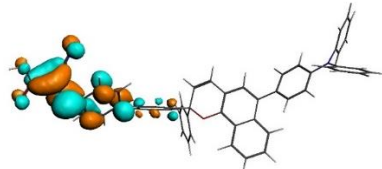
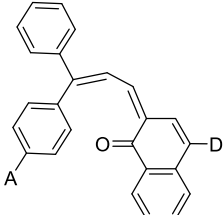
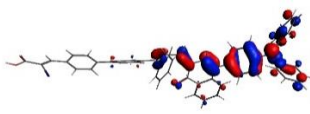
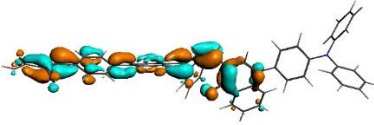


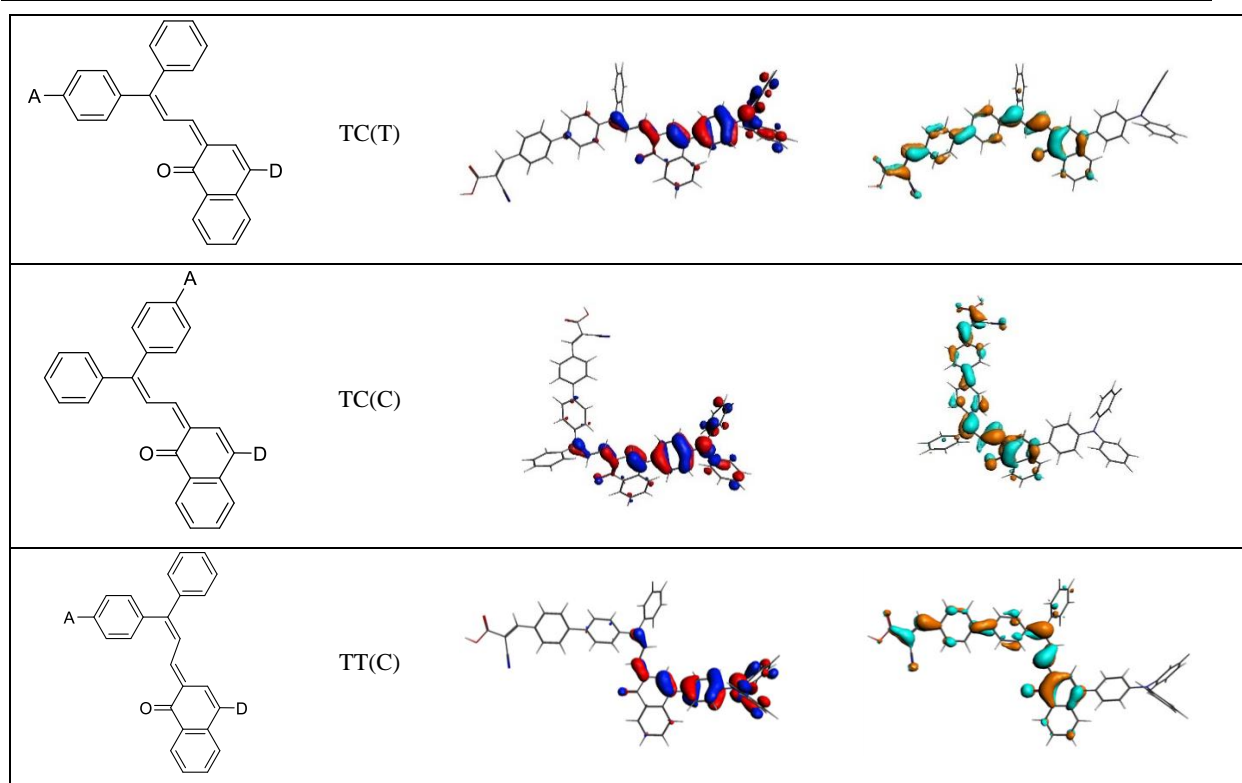
Supplementary Table 5. Relative energies ΔE_{SP} (kcal/mol) calculated at the B3LYPD3/TZ2P/COSMO level, eigenvalues of HOMO and LUMO, energy gap (eV) for the CF and OF geometries of NPB.

	Form	ΔE_{SP}	HOMO	LUMO	gap
	CF	0.0	-5.13	-2.92	2.21
	CC(T)	2.9	-5.15	-3.22	1.93

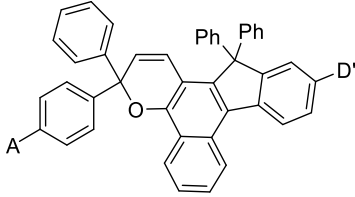
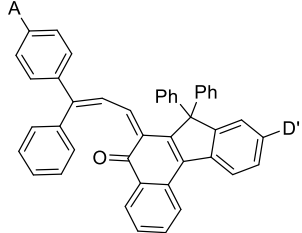
	TC(T)	-0.25	-5.16	-3.29	1.87
	TC(C)	1.17	-5.17	-3.24	1.93
	TT(C)	-3.3	-5.22	-3.24	1.98

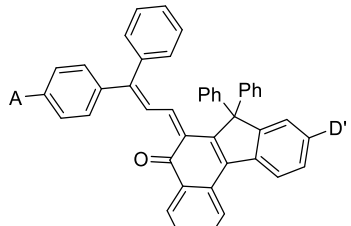
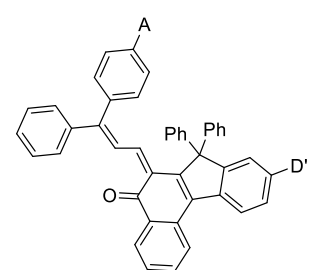
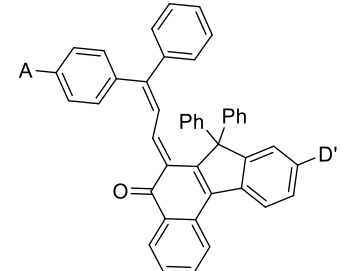
Supplementary Table 6. HOMO and LUMO localization for the CF and OF geometries of **NPB**, from the B3LYP single-points.

Form	HOMO	LUMO
		
		

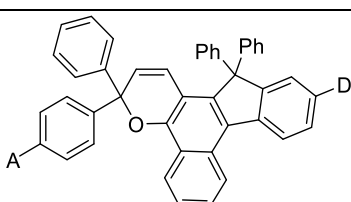
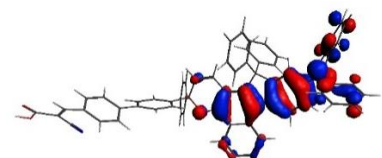
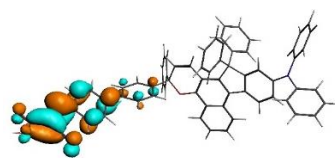
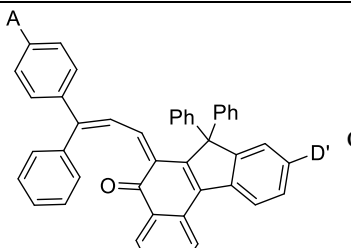
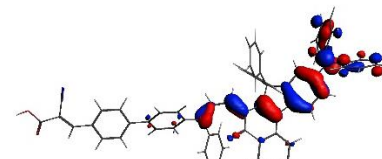
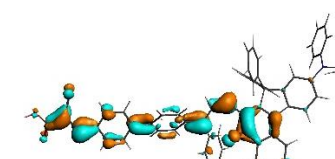


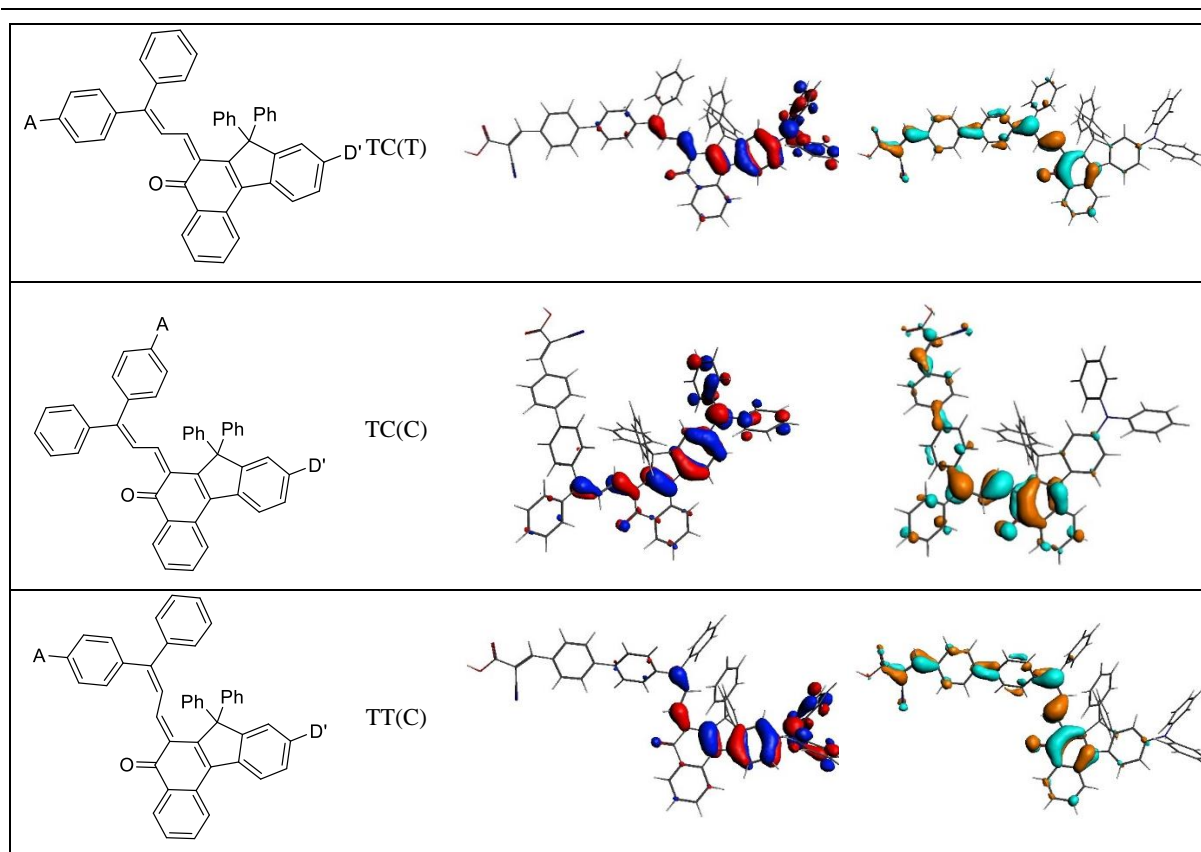
Supplementary Table 7. Relative energies ΔE_{SP} (kcal/mol) calculated at the B3LYPD3/TZ2P/COSMO level, eigenvalues of HOMO and LUMO, energy gap (eV) for the CF and OF geometries of **NPI** (D' = diphenylamine).

	Form	ΔE_{SP}	HOMO	LUMO	gap
	CF	0	-5.07	-2.96	2.11
	CC(T)	9.76	-5.08	-3.21	1.87

	TC(T)	-3.97	-5.09	-3.28	1.86
	TC(C)	-1.41	-5.09	-3.23	1.81
	TT(C)	7.71	-5.11	-3.24	1.88

Supplementary Table 8. HOMO and LUMO localization for the CF and OF geometries of NPI (D'= diphenylamine) from the B3LYP single-points.

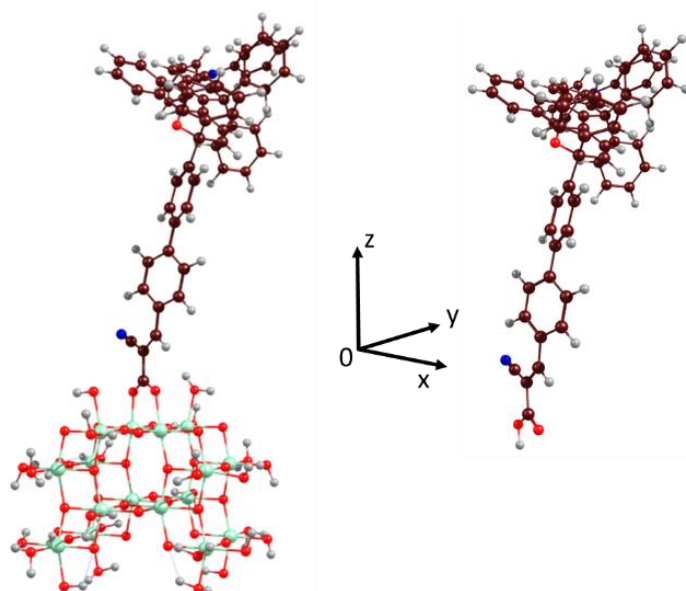
Form	HOMO	LUMO
 CF		
 CC(T)		



Supplementary Table 9. Dipole moment (Debye) and its three components, according to a reference frame with z perpendicular to the surface of TiO_2 as shown in **Supplementary Figure 3**.

Dye (opt. geometry)	form	μ_x	μ_y	μ_z	μ
NPI (on TiO_2)	CF	-4.9	-0.9	1.0	5.1
	OF TC(T)	-9.3	-0.6	5.1	10.6
	OF TT(C)	-7.9	-3.1	5.6	10.2
NPI (isolated)	CF	6.1	0.8	1.8	6.5
	OF TC(T)	9.2	0.8	5.1	10.6
	OF TT(C)	9.5	2.4	6.3	11.7
NPB (isolated)	CF	3.4	1.3	3.6	5.1
	OF TC(T)	9.7	3.0	5.7	11.6
	OF TT(C)	9.1	2.0	5.4	10.8

NPL (isolated)	CF	-9.0	1.1	5.8	10.8
	OF TC(T)	-5.1	-0.7	8.2	9.7
	OF TT(C)	-5.9	-0.9	9.3	11.1



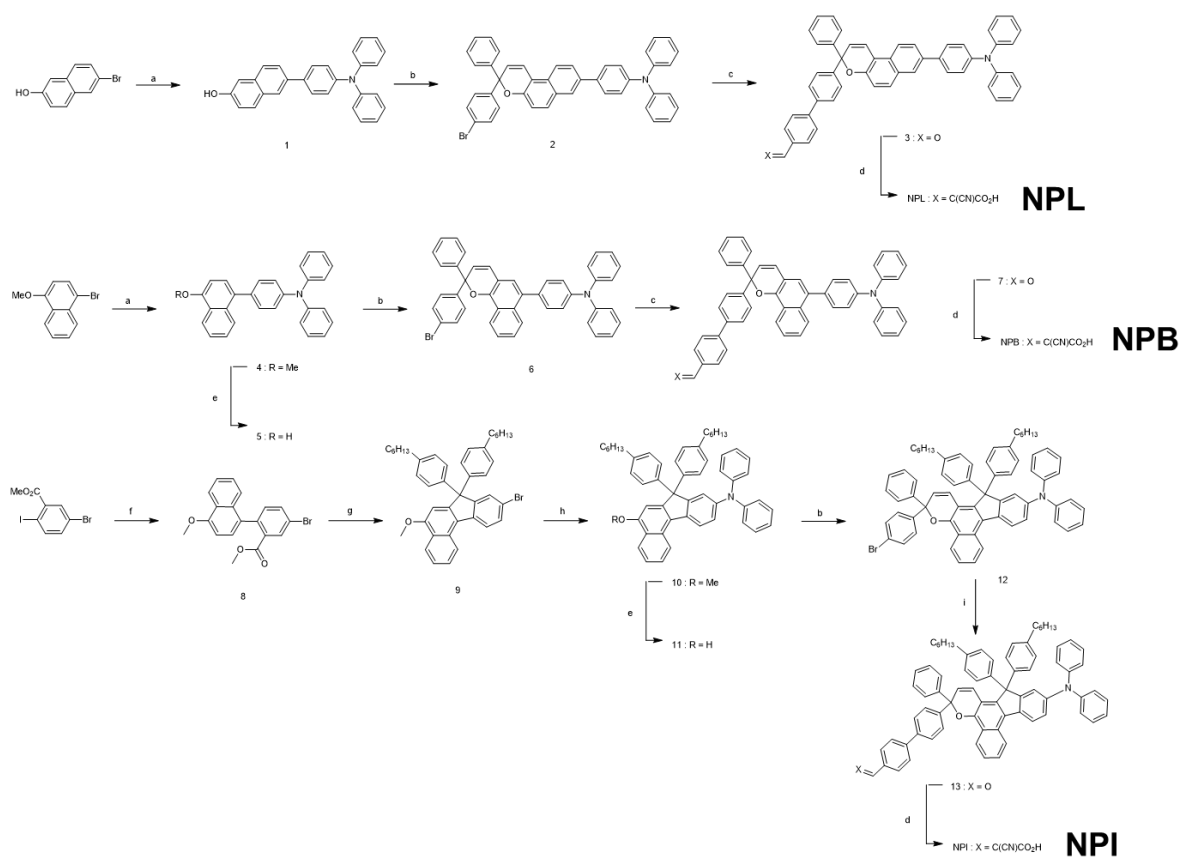
Supplementary Figure 3. Left: **NPI** in CF on TiO_2 model; middle: reference frame for calculating dipole moment components; right: isolated molecule for calculation of dipole moment. The xOz plane contains the acrylic group. (Oxygen : red, Nitrogen: blue, Titanium: green, Carbon: brown, Hydrogen: grey)

Supplementary Note 2

The critical step in the synthesis of the photochromic dyes is the formation of the naphthopyran ring. This condensation reaction involves a Claisen rearrangement of the alkynyl-aryl ethers resulting from the O-alkylation of the naphthol with aryl-propargylic alcohol, followed by a proton shift and an electrocyclic ring closure. This reaction is performed under catalytic acidic conditions, and as acidic reagent, we selected PPTS (pyridinium para-toluene sulfonate).⁴⁹ The choice of a weakly acid catalyst is crucial to reduce the degradation of the aryl-propargylic alcohol, which is unstable to stronger acid conditions and can undergo a Meyer-Shuster rearrangement.⁴⁹

The synthesis of **NPL** and **NPB** is achieved in 4 and 5 steps respectively starting from the brominated naphth-2-ol or methyl-protected brominated 1-naphthol. The methyl-protection of the 4-bromo-naphth-1-ol is mandatory, because such derivatives can rapidly convert into

naphthoquinone. For these two dyes, the triphenylamine unit was introduced on the naphthols via a Suzuki cross-coupling reaction in good yields. The resulting compounds **1** and **5** are converted into photochromic dyes **2** and **6** respectively during the chromenisation reaction. Then, *para*-phenyl-carboxaldehyde is introduced on the molecules yielding the intermediates **3** and **7** that are subsequently converted through a Knoevenagel condensation into the corresponding dyes **NPL** and **NPB**. The synthesis of **NPI** is a bit longer since it first requires the preparation of the indeno-fused protected naphthol derivative, compound **9**. The introduction of the diphenylamino unit to give compound **10** is performed via a Buchwald cross-coupling reaction. After deprotection of the hydroxyl function, compound **11** is involved in the condensation reaction to form the indeno-fused naphthopyran derivate **12**. The introduction of the *para*-phenyl-carboxaldehyde followed by the Knoevenagel condensation with cyanoacrylic acid affords **NPI**. The synthetic routes for the preparation of the three photochromic dyes are presented in **Supplementary Figure 4**



- (4-(diphenylamino)phenyl)boronic acid, K_3PO_4 , $Pd(OAc)_2$, $iPrOH/H_2O$ 2/1 (v/v), $110^\circ C$, 75% (**1**), 97% (**4**);
- 1-(4-(diphenylamino)phenyl)-1-phenylprop-2-yn-1-ol, PPTS, trimethylorthoformate, DCE, $80^\circ C$, 60% (**2**), 40% (**6**), 47% (**12**);
- 4-(4,4,5,5-tetramethyl-1,3,2-dioxaborolan-2-yl)-benzaldehyde, $Pd(PPh_3)_4$, K_2CO_3 , THF/ H_2O , $80^\circ C$, 75% (**3**), 80% (**7**);
- Cyanoacetic acid, piperidine, MeCN/ $CHCl_3$, $80^\circ C$, 75% (NPL), 80% (NPB), 88% (NPI);
- BBr_3 , DCM, RT, 80% (**5**), 97% (**11**);
- (4-methoxynaphthalen-1-yl)zinc(II) bromide, $Pd(PPh_3)_4$, RT, 90%;
- (4-hexylphenyl)lithium, THF, $-95^\circ C$ to RT; then aq. 1M HCl, THF, RT; then $BF_3 \cdot OEt_2$, $CHCl_3$, RT; 53% over three steps;
- Diphenylamine, $Pd_2(dba)_3$, tBuOK, toluene, $110^\circ C$, 68%;
- (4-(diphenylamino)phenyl)boronic pinacol ester, $Pd(dppf)Cl_2$, AcOK, 1,4-dioxane, $80^\circ C$, 75%.

Supplementary Figure 4. Synthetic routes to access to the photochromic photosensitizers **NPL**, **NPB** and **NPI**.

Supplementary methods

Synthesis of Compound 1.

2-bromo-6-naphtol (1.00 g, 4.5 mmol, 1.00 eq), 4-diphenylamino-phenylboronic acid (1.69 g, 5.8 mmol, 1.30 eq), K_3PO_4 (2.85 g, 13.4 mmol, 3.00 eq) and $Pd(OAc)_2$ (20.1 mg, 89 μ mol, 2.0 mol%) are dissolved in a mixture of *i*PrOH and H_2O (2:1 respectively, 150 mL). The mixture is stirred for 2 hours at 110°C before being cooled down to room temperature. The organic phase is extracted with EtOAc, dried on sodium sulfate and concentrated under vacuum. Purification on silica gel using *n*-hexane/EtOAc (7:3) as eluent afford pure compound **1** as a white solid (1.30 g, 3.4 mmol, 75 %). **1H NMR (CD_2Cl_2 , 400MHz) δ (ppm):** 7.95 (s, 1H), 7.79 (d, 1H, $^3J = 8.8$ Hz), 7.74 (d, 1H, $^3J = 8.6$ Hz), 7.69 (dd, 1H, $^3J = 8.6$ Hz, $^4J = 1.8$ Hz), 7.60 (d, 2H, $^3J = 8.6$ Hz), 7.28 (dd, 4H, $^3J_1 = 7.5$ Hz, $^3J_2 = 8.3$ Hz), 7.18-7.08 (m, 8H), 7.04 (t, 2H, $^3J = 7.3$ Hz), 5.14 (s, 1H). **^{13}C NMR (CD_2Cl_2 , 100MHz) δ (ppm):** 153.6, 147.7, 147.1, 135.7, 134.9, 133.6, 123.0, 129.3, 129.2, 127.7, 126.8, 125.8, 124.8, 124.4, 124.0, 123.0, 118.1, 109.2. **HRMS (ESI - TOF):** calcd. for $C_{28}H_{21}NO$, 387.1623; found 387.1623.

Synthesis of Compound 2

Compound **1** (400 mg, 1.03 mmol, 1.00 eq), 1-(4-bromophenyl)-1-phenylprop-2-yn-1-ol (445 mg, 1.55 mmol, 1.50 eq), PPTS (13 mg, 52 μ mol, 5.0mol%) are dissolved in anhydrous 1,2-dichloroethane (5.0 mL). Trimethyl orthoformate (0.25 mL, 2.1 mmol, 2.0 eq) is added and the reaction is heated to reflux for 9 hours. The solvent is removed under reduced pressure and the

resulting crude product is purified on silica gel using (n-hexane:DCM, 7:3) to afford compound **2** a white solid (400 mg, 0.60 mmol, 60%). **¹H NMR (CD₂Cl₂, 400MHz) δ (ppm):** 8.06 (d, 1H, ³J = 8.9Hz), 7.97 (d, 1H, ⁴J = 1.7Hz), 7.80 (dd, 1H, ³J = 9.0Hz, ⁴J = 2.0Hz), 7.77 (d, 1H, ³J = 9.3 Hz), 7.64 (d, 2H, ³J = 8.7 Hz), 7.55-7.44 (m, 5H), 7.44-7.29 (m, 9H), 7.26 (d, 1H, ³J = 8.8 Hz), 7.22-7.14 (m, 6H), 7.09 (tt, 2H, ³J = 7.3 Hz, ⁴J = 1.0 Hz), 6.33 (d, 1H, ³J = 9.9 Hz). **¹³C NMR (CD₂Cl₂, 100MHz) δ (ppm):** 150.2, 147.7, 147.2, 144.3, 144.0, 135.9, 134.5, 131.2, 130.2, 129.8, 129.3, 128.8, 128.6, 128.2, 127.7, 127.6, 127.5, 126.8, 126.0, 125.4, 124.4, 123.9, 123.0, 121.9, 121.5, 120.1, 118.5, 114.1. **HRMS (ESI - TOF):** calcd. for C₄₃H₃₀BrNO, 655.1511; found 655.1504.

Synthesis of Compound **3**

Compound **2** (100 mg, 0.15 mmol), 4-(4,4,5,5-tetramethyl-1,3,2-dioxaborolan-2-yl)-benzaldehyde (53 mg, 0.22 mmol, 1.50 eq), Pd(PPh₃)₄ (4.0 mg, 3.1 μmol, 2.0 mol%) are dissolved in a mixture of THF (10 mL) and an aqueous solution of K₂CO₃ (0.5M, 0.8 mL, 2.7 eq). The mixture is stirred at 80°C for 16 hours. The reaction is cooled down to room temperature. The mixture is extracted with diethyl ether (2 x 15 mL). The combined organic layer is washed with brine, dried on sodium sulfate and concentrated under reduced pressure. The resulting crude product is purified on silica gel (DCM:petroleum ether, 7:3) to afford compound **3** as a white solid (78 mg, 0.11 mmol, 75 %). **¹H NMR (CD₂Cl₂, 400MHz) δ (ppm):** 10.06 (s, 1H), 8.08 (d, 1H, ³J = 8.9 Hz), 7.98-7.94 (m, 3H), 7.83-7.76 (m, 4H), 7.67 (s, 4H), 7.64 (d, 2H, ³J = 8.7 Hz), 7.61-7.57 (m, 2H), 7.45 (d, 1H, ³J = 10.0 Hz), 7.43-7.37 (m, 2H), 7.36-7.28 (m, 6H), 7.21-7.14 (m, 6H), 7.09 (tt, 2H, ³J = 7.3 Hz, ⁴J = 1.0 Hz), 6.43 (d, 1H, ³J = 9.9 Hz). **¹³C NMR (CDCl₃, 100MHz) δ (ppm):** 191.8, 150.5, 147.8, 147.2, 146.5, 145.2, 144.6, 138.8, 135.9, 135.2, 134.7, 130.3, 130.2, 129.8, 129.4, 128.8, 128.3, 127.8, 127.76, 127.71, 127.60, 127.57, 127.2, 127.0, 126.1, 125.7, 124.5, 124.0, 123.0, 122.0, 120.0, 118.7, 114.1, 82.4.

Synthesis of Compound **NPL**

Compound **3** (30 mg, 44 μmol, 1.0 eq), cyanoacetic acid (19 mg, 0.22 mmol, 5.00 eq) are dissolved in a mixture of acetonitrile and chloroform (8 and 5 mL, respectively). A catalytic amount of piperidine is added and the reaction mixture is heated at 80°C for 3 hours. Solvents are removed under reduced pressure and the crude product is solubilized in chloroform (20 mL).

The organic phase is washed with an aqueous HCl solution (2 M, 2 x 10 mL), dried on sodium sulfate and concentrated. The crude solid is purified on silica gel (DCM, DCM/MeOH 98/2 to DCM/MeOH/AcOH 96/2/2) to afford compound **NPL** as a pale yellow solid (24 mg, 33 μ mol, 75%). **¹H NMR (THF-*d*₈, 400MHz) δ (ppm):** 8.19 (bs, 1H), 8.08 (d, ³*J* = 8.9 Hz, 1H), 8.04 (bs, 1H), 7.96 (s, 1H), 7.75 (t, ³*J* = 9.3 Hz, 3H), 7.61-7.66 (m, 6H), 7.54 (d, ³*J* = 7.8 Hz, 2H), 7.46 (d, ³*J* = 10.0 Hz, 1H), 7.30 (t, ³*J* = 7.6 Hz, 2H), 7.20-7.26 (m, 6H), 7.08-7.13 (m, 6H), 6.99 (t, ³*J* = 7.1 Hz, 2H), 6.41 (d, ³*J* = 10.0 Hz, 1H). **¹³C NMR (THF-*d*₈, 100MHz) δ (ppm):** 171.2, 153.3, 151.3, 148.6, 148.0, 146.3, 145.8, 145.3, 140.3, 139.3, 136.5, 135.7, 132.0, 131.9, 130.8, 130.7, 129.9, 129.6, 128.7, 128.5, 128.3, 128.2, 128.1, 128.0, 127.9, 127.7, 127.5, 127.4, 127.3, 126.4, 126.1, 124.9, 124.8, 123.5, 122.7, 120.4, 119.1, 116.5, 114.9. **HRMS (ESI - TOF):** calcd. for C₅₃H₃₆N₂O₃, 748.2720; found 748.2729.

Synthesis of Compound 4

1-methoxy-6-bromonaphtalene (790 mg, 3.30 mmol, 1.00 eq) and 4-diphenylamino-phenylboronic acid (1.60 g, 4.33 mmol, 1.00 eq), K₃PO₄ (2.12 g, 10.0 mmol) and Pd(OAc)₂ (15.0 mg, 67 μ mol, 2.0 mol%) are dissolved in a mixture of ⁱPrOH and H₂O (2:1, 150 mL). The mixture is heated at reflux for 2 hours before being cooled down to room temperature. The organic phase was extracted with EtOAc (20 mL), dried on sodium sulfate and concentrated under vacuum. Purification on silica gel (*n*-hexane:EtOAc, 95:5) as eluent affords compound **4** as a white solid (1.30 g, 3.2 mmol, 97%). **¹H NMR (CD₂Cl₂, 400 MHz, 298 K) δ (ppm):** 8.33-8.29 (m, 1H), 7.98-7.94 (m, 1H), 7.51-7.45 (m, 2H), 7.37-7.34 (m, 3H), 7.32-7.17 (m, 4H), 7.18-7.15 (m, 5H), 7.10 (dd, 1H, ³*J* = 8.1 Hz, ⁴*J* = 2.8 Hz), 7.05 (td, 2H, ³*J* = 7.9 Hz, ⁴*J* = 1.0 Hz), 6.90 (d, 2H, ³*J* = 7.9 Hz), 4.08 (s, 3H). **¹³C NMR (CD₂Cl₂, 100 MHz) δ (ppm):** 155.2, 148.3, 147.1, 135.4, 132.9, 132.6, 131.4, 129.7, 127.6, 127.4, 127.2, 126.8, 126.1, 125.46, 124.7, 124.4, 124.0, 123.3, 122.5, 104.0, 56.0. **Elemental Analysis** (calcd, found for C₂₉H₂₃NO): C (86.75, 86.82), H (5.77, 5.75), N (3.49, 3.54).

Synthesis of Compound 5

Compound **4** (0.50 g, 1.2 mmol, 1.0 eq) is dissolved in anhydrous DCM (10 mL). BBr₃ (1.0 M in DCM, 1.6 mL, 1.6 mmol, 1.30 eq) is added at 0°C. The reaction is allowed to warm up at room temperature and is further stirred at this temperature for 3 hours. Saturated aqueous K₂CO₃ solution (20 mL) is added. The organic phase was extracted with DCM (50 mL), dried on sodium sulfate and concentrated under vacuum. Purification on silica gel (*n*-hexane:EtOAc, 8:2) affords compound **5** as a white solid (0.38 g, 1.0 mmol, 80%). **¹H NMR (CD₂Cl₂,**

400MHz) δ (ppm): 8.28-8.26 (m, 1H), 8.02-8.00 (m, 1H), 7.56-7.49 (m, 2H), 7.39-7.30 (m, 7H), 7.24-7.17 (m, 6H), 7.09 (tt, 2H, $^3J=7.3\text{Hz}$, $^4J=1.0\text{Hz}$), 6.94 (d, 2H, $^3J=7.7\text{Hz}$), 5.49(s, 1H). **^{13}C NMR (CD_2Cl_2 , 100MHz) δ (ppm):** 151.2, 148.2, 147.2, 135.3, 133.1, 131.4, 129.7, 127.2, 126.9, 126.3, 125.5, 124.7, 124.0, 123.3, 122.2, 108.6.

Synthesis of Compound 6

Compound **5** (370 mg, 0.95 mmol, 1.00 eq), 1-(4-bromophenyl)-1-phenylprop-2-yn-1-ol (411 mg, 1.43 mmol, 1.50 eq), PPTS (12 mg, 52 μmol , 5.5 mol%) are dissolved in anhydrous 1,2-dichloroethane (6.0 mL). Trimethyl orthoformate (0.21 mL, 1.91 mmol, 2.00eq) is added and the reaction is heated to reflux for 9 hours. Solvents are removed under reduced pressure and the crude solid is purified on silica gel (*n*-hexane:DCM, 6:4) to afford compound **6** as a white solid (250 mg, 0.38 mmol, 40%). **^1H NMR (CD_2Cl_2 , 400MHz) δ (ppm):** 8.45 (d, 1H, $^3J=8.0$ Hz), 7.96 (d, 1H, $^3J=8.4$ Hz), 7.62-7.44 (m, 9H), 7.41-7.30 (m, 9H), 7.24-7.16 (m, 6H), 7.09 (tt, 2H, $^3J=7.3$ Hz, $^4J=0.9$ Hz), 6.86 (d, 1H, $^3J=9.7$ Hz), 6.28 (d, 1H, $^3J=9.7$ Hz). **^{13}C NMR (CD_2Cl_2 , 100MHz) δ (ppm):** 148.2, 147.3, 147.2, 145.0, 144.7, 134.8, 133.5, 133.1, 131.7, 131.6, 131.3, 129.7, 129.1, 128.8, 128.7, 128.3, 128.2, 127.8, 127.1, 126.94, 126.90, 126.5, 126.1, 125.7, 125.2, 124.8, 124.7, 123.8, 123.3, 122.3, 122.0, 83.2, 78.4. **Elemental Analysis** (calcd, found for $\text{C}_{43}\text{H}_{30}\text{BrNO}$): C (78.66, 77.53), H (4.61, 4.62), N (2.13, 1.92).

Synthesis of Compound 7

Compound **6** (180 mg, 0.27 mmol, 1.00 eq), 4-(4,4,5,5-tetramethyl-1,3,2-dioxaborolan-2-yl)-benzaldehyde (70 mg, 0.30 mmol, 1.1 eq), $\text{Pd}(\text{PPh}_3)_4$ (9.5 mg, 8.2 μmol , 3.0 mol%) are dissolved in a mixture of THF (10 mL) and an aqueous solution of K_2CO_3 (0.5M, 1.6 mL, 0.80 mmol, 3.0 eq). The mixture is heated at reflux for 18 hours. The reaction is cooled down to room temperature, and diluted with water (20 mL) and diethyl ether (20 mL). The aqueous layer is extracted with diethyl ether (20 mL). The combined organic layer is washed with brine, dried on sodium sulfate and concentrated under reduced pressure. The resulting crude product is purified on silica gel (DCM:petroleum ether, 7:3) to afford compound **7** as a white solid (150 mg, 0.22 mmol, 80%). **^1H NMR (CD_2Cl_2 , 400MHz) δ (ppm):** 10.02 (s, 1H), 8.48 (d, 1H, $^3J=8.3$ Hz), 7.94 – 7.88 (m, 3H), 7.74 – 7.66 (m, 4H), 7.63-7.60 (m, 4H), 7.54 (t, 1H, $^3J=7.6$ Hz), 7.47 – 7.42 (m, 1H), 7.37 (t, $^3J=7.5$ Hz, 2H), 7.33-7.28 (m, 7H), 7.18-7.18 (m, 7H), 7.05 (t, 2H, $J=7.3$ Hz), 6.84 (d, 1H, $^3J=9.7$ Hz), 6.33 (d, 1H, $^3J=9.7$ Hz). **^{13}C NMR (CD_2Cl_2 , 100MHz) δ (ppm):** 192.1, 147.3, 147.2, 146.7, 145.9, 145.4, 139.4, 135.8, 134.9, 133.4, 133.1, 131.3, 130.5, 129.7, 128.7, 128.1, 128.0, 128.0, 127.8, 127.6, 127.1, 126.9, 126.5, 126.1, 125.7,

124.8, 124.6, 123.8, 123.3, 122.4, 115.8, 83.4. **Elemental Analysis** (calcd, found for C₅₀H₃₅NO₂): C (88.08, 87.11), H (5.17, 5.03), N (2.05, 1.98).

Synthesis of Compound NPB

Compound **6** (230 mg, 0.34 mmol, 1.00 eq), cyanoacetic acid (143 mg, 1.69 mmol, 5.00 eq) are solubilized in a mixture of acetonitrile (8.0 mL) and chloroform (12 mL). A catalytic amount of piperidine was added and the reaction mixture was refluxed for 3 hours. Solvent was removed under reduced pressure and the solid redissolved in chloroform. The organic phase was washed with a HCl solution (2 M), dried on sodium sulfate and concentrated. The crude solid was chromatographed on silica using DCM followed by DCM/MeOH and DCM/MeOH/Acetic acid 96/2/2 as eluents to afford compound **NPB** as a pink solid (204 mg, 0.26 mmol, 80%). **¹H NMR (THF-*d*₈, 400MHz) δ (ppm):** 8.45 (d, 1H, ³*J* = 7.9 Hz), 8.26 (s, 1H), 8.11 (d, 2H, ³*J* = 8.5 Hz), 7.87 (d, 1H, ³*J* = 8.4 Hz), 7.79 (d, 2H, ³*J* = 8.4 Hz), 7.69 (s, 4H), 7.62 – 7.57 (m, 2H), 7.48 (ddd, 1H, ³*J*₁ = 8.2, ³*J*₂ = 6.8, ⁴*J* = 1.1 Hz), 7.39 (ddd, 1H, ³*J*₁ = 8.2, ³*J*₂ = 6.8, ⁴*J* = 1.3 Hz), 7.34 – 7.20 (m, 9H), 7.17 (s, 1H), 7.15 – 7.09 (m, 6H), 7.03 – 6.97 (m, 2H), 6.84 (d, ³*J* = 9.8 Hz, 1H), 6.37 (d, ³*J* = 9.7 Hz, 1H). **¹³C NMR (THF-*d*₈, 100MHz) δ (ppm):** 163.7, 153.7, 148.7, 147.7, 146.5, 146.0, 145.5, 139.4, 132.1, 131.5, 129.9, 128.8, 128.4, 128.2, 128.1, 128.0, 127.5, 127.4, 126.1, 125.1, 124.5, 124.1, 123.5, 116.2, 116.0, 104.3, 83.9. **HRMS (ESI - TOF):** calcd. for C₅₃H₃₆N₂O₃, 748.2720; found 748.2717. **Elemental Analysis** (calcd, found for C₅₃H₃₆N₂O₃): C (85.00, 83.70), H (4.85, 4.68), N (3.74, 3.64).

Synthesis of Compound 8

To a solution of 1-bromo-4-methoxynaphthalene (4.00 g, 16.8 mmol, 1.00 eq) in degassed and anhydrous THF (100 mL) is added dropwise at -78°C *n*-BuLi (2.5 M in hexanes, 7.1 mL, 17.7 mmol, 1.05 eq). The reaction mixture is stirred at -78°C for 1 hour before a solution of ZnBr₂ (4.18 g, 18.5 mmol, 1.10 eq) in anhydrous THF (20 mL) is added dropwise. The mixture is allowed to warm up to 0°C and is further stirred at this temperature for 1 hour. Methyl-5-bromo-2-iodobenzoate (5.18 g, 15.1 mmol, 0.90 eq) and Pd(PPh₃)₄ (670 mg, 0.579 mmol, 4.0 mol%) are successively added and the mixture is allowed to warm up at room temperature and is stirred at room temperature for 20 hours. The reaction mixture is poured on 2M aqueous HCl (20 mL) and diluted with diethyl ether (50 mL). The organic layer is washed with water and brine, dried over Na₂SO₄, filtered off and concentrated under vacuum. The resulting crude product is purified by column chromatography (SiO₂, petroleum ether/DCM 7/3 to 65/35). Final purification is achieved by recrystallization from *n*-hexane (150 mL). Filtration affords pure

compound **11** as white crystals (5.11 g, 13.7 mmol, 90%). **¹H NMR (CD₂Cl₂, 400MHz) δ (ppm):** 8.30 (d, 1H, ³J = 8.3 Hz), 8.10 (d, 1H, ³J = 2.0 Hz), 7.68 (dd, 1H, ³J = 8.2 Hz, ⁴J = 2.1 Hz), 7.44 (m, 1H), 7.37 (m, 2H), 7.26 (s, 1H), 7.00 (d, 2H, ³J = 7.85 Hz), 4.02(s, 3H), 3.39(s, 3H). **¹³C NMR (CDCl₃, 100MHz) δ (ppm):** 166.8, 155.3, 140.4, 134.6, 134.0, 132.9, 132.8, 130.6, 126.8, 126.1, 125.5, 125.2, 125.1, 122.4, 121.3, 103.2, 55.6, 52.2. **Elemental analysis** (calcd., found for C₁₉H₁₅Br₂O₃): C (61.47, 61.29), H (4.07, 3.97).

Synthesis of Compound 9

To a solution of 1-Bromo-4-hexylbenzene (4.21 g, 17.5 mmol, 2.40 eq) in anhydrous THF (80 mL) is added dropwise at -95°C n-BuLi (2.5 M in hexane, 7.0 mL, 17.50 mmol, 2.40 eq). The reaction is stirred at this temperature for 45 min before Compound **8** (2.70 g, 7.27 mmol, 1.00 eq) is added in one portion as a solid. The mixture is further stirred at this temperature for 30 min and then allowed to reach RT overnight (19 h). The reaction mixture is poured on HCl 2 M (30 mL), diluted in Et₂O (100 mL) and the mixture is stirred at RT 10 min. The organic layer is washed with water and brine, dried over Na₂SO₄, filtered off and concentrated under vacuum. The resulting orange oil is purified by column chromatography (PE/DCM 8/2 to PE/DCM 7/3) to obtain an intermediate alcohol (3.54 g, 5.33 mmol, 1.00 eq).

The intermediate alcohol (3.54 g, 5.33 mmol, 1.00 eq) is dissolved in anhydrous chloroform (150 mL) and BF₃.OEt₂ (1.3 mL, 1.54 g, 10.7 mmol, 2.00 eq) is added dropwise at room temperature. The reaction mixture is stirred 1h30. Water (100 mL) is added and the mixture is stirred at room temperature for 10 minutes. The layers are separated. The organic layer is washed with water and brine, dried over Na₂SO₄, filtered off and concentrated to dryness. The resulting oil is purified by column chromatography (neat PE to PE/DCM 95/5) to afford compound **9** as a colourless oil (2.52 g, 3.90 mmol, 73%). **¹H-NMR (CDCl₃, 298 K, 400 MHz) δ (ppm)** 8.61 (d, ³J = 8.4 Hz, 1H), 8.34 (dd, ³J = 8.5, 0.9 Hz, 1H), 8.10 (d, ³J = 8.0 Hz, 1H), 7.67 (ddd, ³J₁ = 8.4, ³J₂ = 6.9, ⁴J = 1.4 Hz, 1H), 7.55 – 7.48 (m, 3H), 7.26 (s, 2H), 7.10 (d, ³J = 8.4 Hz, 4H), 7.04 (d, J = 8.4 Hz, 4H), 6.83 (s, 1H), 3.91 (s, 3H), 2.57 – 2.52 (m, 4H), 1.62 – 1.54 (m, 4H), 1.37 – 1.24 (m, 12H), 0.90 – 0.84 (m, 6H). **¹³C-NMR (CDCl₃, 298 K, 100 MHz) δ (ppm):** 156.2, 154.9, 151.5, 142.0, 141.7, 140.7, 130.5, 130.2, 129.1, 128.5, 128.3, 127.7, 126.1, 125.9, 125.2, 123.7, 123.4, 123.3, 119.4, 102.3, 55.8, 35.7, 31.8, 31.4, 29.3, 22.7, 14.2. **HRMS (ESI-TOF):** calcd. for C₄₂H₄₅BrO, 644.2648; found 644.2649.

Synthesis of Compound 10

To a solution of compound **9** (895 mg, 1.38 mmol, 1.00 eq) in anhydrous toluene (20 mL) are added diphenylamine (258 mg, 1.52 mmol, 1.10 eq), Pd₂(dba)₃ (25.3 mg, 27.7 μmol, 2.0 mol%), HP^tBu₃BF₄ (32 mg, 11 μmol, 8.0 mol%) and potassium tert-butoxide (466 mg, 4.15 mmol, 3.00 eq). The reaction mixture is stirred at 110°C for 20 hours. The reaction mixture is poured on water (100 mL), diluted with DCM (50 mL) and the mixture is stirred at room temperature for 10 minutes. The organic layer is washed with water and brine, dried over Na₂SO₄, filtered off and concentrated under vacuum. The resulting crude product is purified by column chromatography (neat PE to PE/DCM 95/5) to afford compound **10** as a white foam (693 mg, 0.944 mmol, 68%). **¹H NMR (CDCl₃, 400 MHz) δ (ppm):** 8.60 (d, 1H, ³J = 8.4 Hz), 8.31 (dd, 1H, ³J = 0.9 Hz, ⁴J = 0.9 Hz), 8.05 (d, 1H, ³J = 8.5 Hz), 7.59 (m, 1H), 7.47 (m, 1H), 7.27 (d, 1H, ³J = 2.2 Hz), 7.17 (m, 4H), 7.10-6.93 (m, 15H), 6.83 (s, 1H), 3.88 (s, 3H), 2.53 (t, 4H), 1.55 (m, 4H), 1.28 (m, 12H), 0.87 (t, 6H). **¹³C NMR (CDCl₃, 100 MHz) δ (ppm):** 155.2, 154.2, 150.6, 147.8, 145.4, 142.6, 141.2, 136.3, 129.9, 129.1, 128.3, 128.2, 127.2, 127.1, 125.7, 124.8, 124.0, 123.8, 123.2, 123.0, 122.6, 122.4, 121.8, 102.6, 65.2, 55.7, 35.6, 31.8, 31.4, 29.2, 22.6, 14.1. **Elemental analysis** (calcd., found for C₅₄H₅₅NO): C (88.36, 88.40), H (7.50, 7.43), N (1.91, 1.70).

Synthesis of Compound 11

A solution of compound **10** (693 mg, 0.944 mmol, 1.00 eq) in anhydrous chloroform (20 mL) is added dropwise at 0°C BBr₃ (1.0 M in DCM, 1.4 mL, 1.4 mmol, 1.5 eq). The reaction mixture is allowed to warm up at room temperature for 20 hours. The reaction mixture is poured on saturated aqueous NaHCO₃ solution (20 mL), diluted with DCM (20 mL) and the mixture is stirred at room temperature for 10 minutes. The aqueous layer is extracted with DCM (20 mL). The combined organic layer is washed with water and brine, dried over Na₂SO₄, filtered off and concentrated under vacuum. The resulting crude product is purified by column chromatography (PE/DCM 7/3 + 1% TEA) to afford compound **11** as a grey foam (606 mg, 0.842 mmol, 89%). **¹H NMR (Acetone-*d*₆, 400 MHz) δ (ppm):** 8.73 (d, 1H, ³J = 8.4 Hz), 8.35 (d, 1H, ³J = 7.6 Hz), 8.23 (d, 1H, ³J = 8.5 Hz), 7.67 (m, 1H), 7.53 (m, 1H), 7.21-7.27 (m, 5H), 6.98-7.09 (m, 16H), 2.55 (t, 4H, ³J = 7.6 Hz), 1.54-1.61 (m, 4H), 1.26-1.36 (m, 12H), 0.97 (t, 6H, ³J = 7.1 Hz). **¹³C NMR (Acetone-*d*₆, 100 MHz) δ (ppm):** 143.1, 131.5, 131.1, 130.0, 129.8, 127.6, 126.7, 125.8, 124.6, 121.9, 119.4, 37.0, 33.4, 33.2, 24.2, 15.3. **HRMS (ESI - TOF):** calcd. for C₅₃H₅₃NO, 719.4121; found 719.4116.

Synthesis of Compound 12

To a solution of compound **11** (600 mg, 0.833 mmol, 1.00 eq) in anhydrous DCE (20 mL) are successively added 1-(4-bromophenyl)-1-phenylprop-2-yn-1-ol (478 mg, 1.67 mmol, 2.00 eq), PPTS (20 mg, 83.3 μ mol, 10 mol%) and trimethylorthoformate (0.17 mL, 1.54 mmol, 2.0 eq). The mixture is stirred at 75°C for 22 hours. 1-(4-bromophenyl)-1-phenylprop-2-yn-1-ol (239 mg, 0.835 mmol, 1.00 eq) is added and the mixture is stirred at 85°C 16 hours more. Once cooled down to room temperature, the reaction mixture is poured on saturated aqueous NaHCO₃ solution (50 mL) and DCM (50 mL) are added. The layers are separated. The organic layer is washed with water, dried over Na₂SO₄, filtered off and concentrated under vacuum. The resulting oil is purified by column chromatography (neat PE to PE/DCM 9/1) to afford compound **12** as a green solid (390 mg, 0.394 mmol, 47%). **¹H NMR (Acetone-d₆, 400 MHz, 298 K) δ (ppm):** 8.71 (d, ³J = 8.5 Hz, 1H), 8.49 (dd, ³J = 8.3, ⁴J = 1.1 Hz, 1H), 8.17 (d, ³J = 8.6 Hz, 1H), 7.63 (ddd, ³J₁ = 8.4, ³J₂ = 6.9, ⁴J = 1.5 Hz, 1H), 7.59 – 7.49 (m, 2H), 7.43 – 7.38 (m, 3H), 7.34 – 7.30 (m, 2H), 7.29 – 7.24 (m, 2H), 7.24 – 7.18 (m, 6H), 7.14 – 7.06 (m, 8H), 7.02 – 6.94 (m, 7H), 6.77 (d, J = 9.8 Hz, 1H), 2.59 (t, J = 7.4 Hz, 4H), 1.64 – 1.55 (m, 4H), 1.39 – 1.24 (m, 12H), 0.85 (t, ³J = 6.0 Hz, 6H). **¹³C NMR (Acetone-d₆, 100MHz, 298K) δ (ppm):** 157.8, 148.6, 148.5, 147.4, 147.0, 144.8, 144.7, 142.4, 142.3, 140.8, 140.6, 136.1, 132.2, 132.1, 130.7, 130.3, 130.0, 129.9, 129.8, 129.6, 129.5, 129.3, 129.2, 129.19, 129.14, 128.9, 128.7, 128.6, 128.2, 127.7, 127.5, 126.6, 126.4, 125.1, 124.2, 124.0, 123.8, 123.3, 122.3, 121.4, 82.8, 80.3, 65.7, 52.8, 36.3, 32.6, 32.42, 32.40, 23.5, 14.66, 14.64. **HRMS (ESI - TOF):** calcd. for C₆₈H₆₂NO⁷⁹Br; 987.4009; found 987.4012.

Synthesis of Compound 13

A solution of compound **12** (189 mg, 0.191 mmol, 1.00 eq) in a mixture of 1,4-dioxane (20 mL) and 1M aqueous AcOK (1.0 mL, 1.0 mmol, 5.0 eq) is degassed 20 minutes by gentle bubbling with Argon. 4-(4,4,5,5-tetramethyl-1,3,2-dioxaborolan-2-yl)-benzaldehyde (55 mg, 0.23 mmol, 1.2 eq) and Pd(dppf)Cl₂ (8.0 mg, 0.010 mmol, 5.0mol%) are successively added and the reaction mixture is stirred at 80°C for 16h. Water (30 mL) and EtOAc (20 mL) are added to the mixture, which is further stirred at room temperature for 10 minutes. The layers are separated and the aqueous layer is extracted once with EtOAc (20 mL). The combined organic layer is dried over Na₂SO₄, filtered off and concentrated under vacuum. The resulting residue is purified by column chromatography (silica gel, PE/DCM 7/3 to 6/4) to afford compound **13** as a green solid (250 mg, 0.246 mmol, 75 %). **¹H NMR (CD₂Cl₂, 400MHz) δ (ppm):** 10.01 (s, 1H), 8.60 (d, 1H, ³J = 8.4 Hz), 8.48 (dd, 1H, J = 8.4 Hz, J = 1.1 Hz), 8.02 (d, 1H, ³J = 8.6 Hz), 7.92 (d, 2H, ³J = 8.4 Hz), 7.67 (d, 2H, ³J = 8.4 Hz), 7.40-7.61 (m, 9H), 7.13-7.28 (m, 13H), 6.93-7.03

(m, 11H), 6.74 (d, 1H, $J = 9.8$ Hz), 5.90 (d, 1H, $J = 9.8$ Hz), 2.59 (m, 4H), 1.59 (m, 4H), 1.30 (m, 12H), 0.85 (t, 6H). ^{13}C NMR (CD_2Cl_2 , 100MHz) δ (ppm): 191.6, 146.4, 141.5, 141.5, 139.6, 139.5, 138.8, 135.4, 130.0, 129.6, 129.1, 129.0, 128.8, 128d.8, 128.1, 128.0, 127.9, 127.6, 127.5, 127.3, 127.0, 126.8, 125.3, 124.2, 124.1, 124.1, 124.0, 123.1, 122.8, 122.7, 120.5, 82.0, 64.6, 35.4, 31.7, 31.5, 29.1, 22.6, 13.8.

Synthesis of Compound NPI

Compound **17** (100 mg, 0.10 mmol, 1.00 eq), freshly recrystallized cyanoacetic acid (83 mg, 0.98 mmol, 9.8 eq) are dissolved in a mixture of acetonitrile (8.0 mL) and chloroform (12 mL). A catalytic amount of piperidine is added and the solution is heated at 80°C for 3 hours. Solvents are removed under reduced pressure and the solid is dissolved back in chloroform. The resulting organic solution is washed with water (20 mL), aqueous 2M HCl solution (20 mL), dried on sodium sulfate and concentrated under vacuum. The resulting green solid is purified by chromatography (silica gel; DCM, then DCM/MeOH 98/2, then and DCM/MeOH/Acetic acid 96/2/2) to afford compound **18** pale green solid (94 mg, 0.09 mmol, 88%). ^1H NMR ($\text{THF}-d_8$, 400MHz) δ (ppm): 8.69 (d, $^3J = 8.6$ Hz, 1H), 8.52 (d, $^3J = 8.1$ Hz, 1H), 8.25 (bs, 1H), 8.16 – 7.99 (m, $^3J = 8.6$ Hz, 3H), 7.76 (bs, 2H), 7.64 – 7.47 (m, 6H), 7.44 (d, $^3J = 7.3$ Hz, 2H), 7.29 – 7.14 (m, 12H), 7.10 – 6.93 (m, 11H), 6.80 (d, $^3J = 9.9$ Hz, 1H), 5.94 (d, $^3J = 9.8$ Hz, 1H), 2.62 (t, $^3J = 6.2$ Hz, 4H), 1.71 – 1.59 (m, 4H), 1.46 – 1.30 (m, 12H), 0.91 (t, $^3J = 6.9$ Hz, 6H). ^{13}C NMR ($\text{THF}-d_8$, 100MHz) δ (ppm): 158.1, 149.0, 147.7, 147.2, 145.6, 142.4, 141.2, 141.2, 139.9, 136.8, 132.6, 131.1, 129.2, 129.2, 129.0, 128.6, 128.4, 128.2, 127.9, 126.9, 126.4, 125.31, 124.30, 123.9, 123.7, 123.6, 122.0, 116.5, 82.1, 36.8, 33.1, 33.0, 30.5, 28.2, 23.2, 14.8. HRMS (ESI-TOF): calcd. for $\text{C}_{78}\text{H}_{68}\text{N}_2\text{O}_3$, 1080.5224; found 1080.5221.

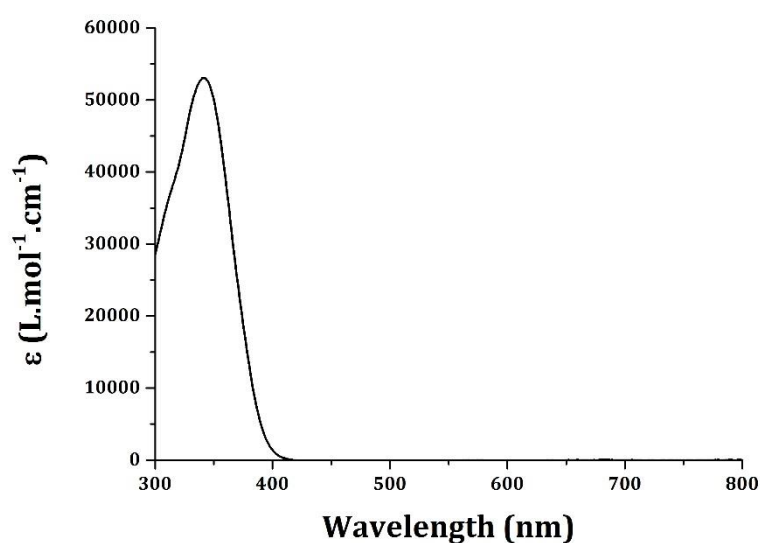
Supplementary Note 3

Within the photochromic naphthopyran dyes, upon UV irradiation of the ring-closed form (CF), heterolytic cleavage of the C-O bond of the pyranic heterocycle occurs and a rearrangement of the pi-conjugated system gives rise to open form isomers (OF) that possess an extended π -conjugated system, thus exhibiting an absorption band in the visible range. The photoisomerism produces several isomers, but all of them are thermally unstable and they can switch

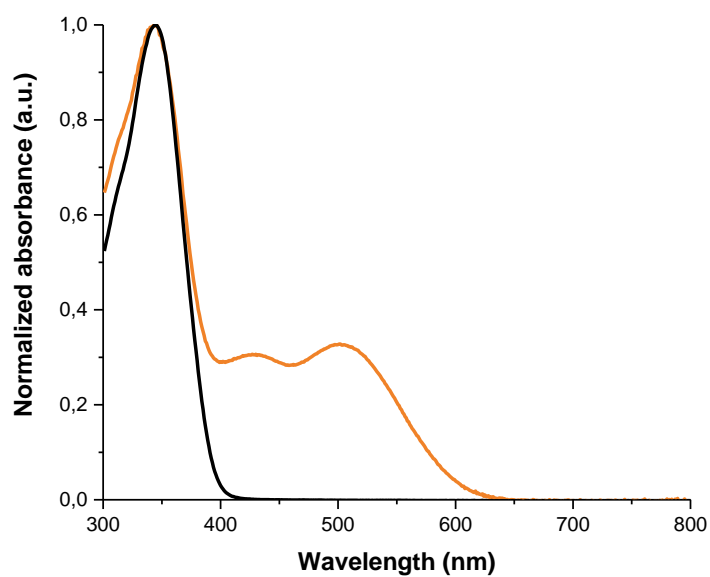
back to their initial form. Consequently, upon irradiation an equilibrium between the closed and opened forms is reached, this is the PhotoStationary State (PSS). The optical parameters of the dyes are reported in **Supplementary Table 10** and the absorption spectra of the three dyes in the dark and under illumination are presented in **Supplementary Figures 5 to 10**.

Dyes	λ_{\max} CF (nm)	λ_{onset} CF (nm)	λ_{\max} OF (nm)	ϵ CF ($\text{M}^{-1} \cdot \text{cm}^{-1}$)	λ_{onset} OF (nm)	ΔE_{opt} OF (eV)	k_1 at 25°C (s^{-1})	k_2 at 25°C (s^{-1})
NPL	345	400	502	$5.3 \cdot 10^4$	618	2.00	$9.8 \cdot 10^{-2}$	$1.1 \cdot 10^{-3}$
NPB	347	400	519	$4.5 \cdot 10^4$	636	1.95	$1.4 \cdot 10^{-3}$	$2.0 \cdot 10^{-4}$
NPI	318	450	605	$4.1 \cdot 10^4$	728	1.70	$2.1 \cdot 10^{-3}$	-

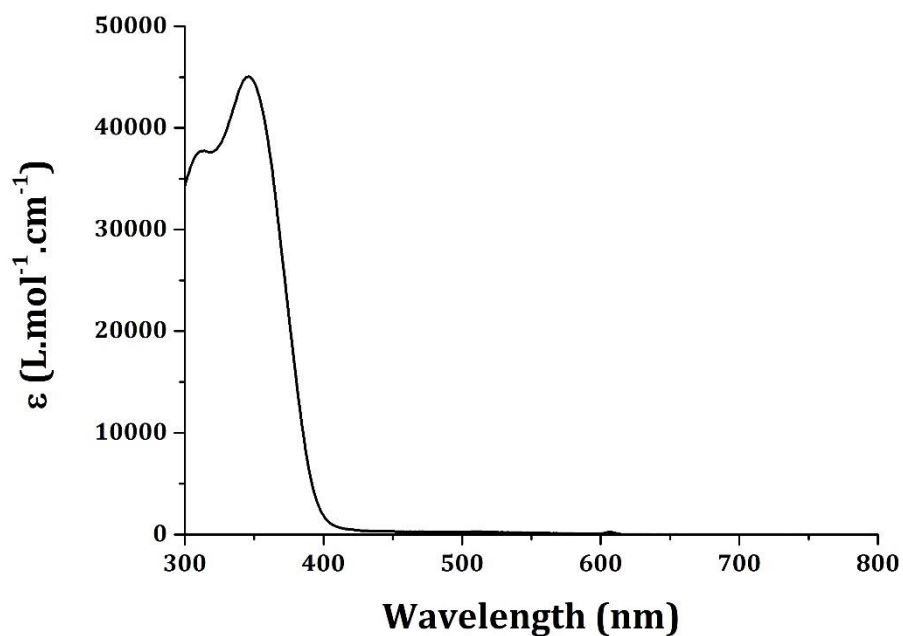
Supplementary Table 10: Optical parameters and kinetics of decolouration measured in toluene (10^{-5} M solutions) in the dark (CF) and under continuous irradiation at 25°C, (OF) conditions with a Xenon lamp (200 W).



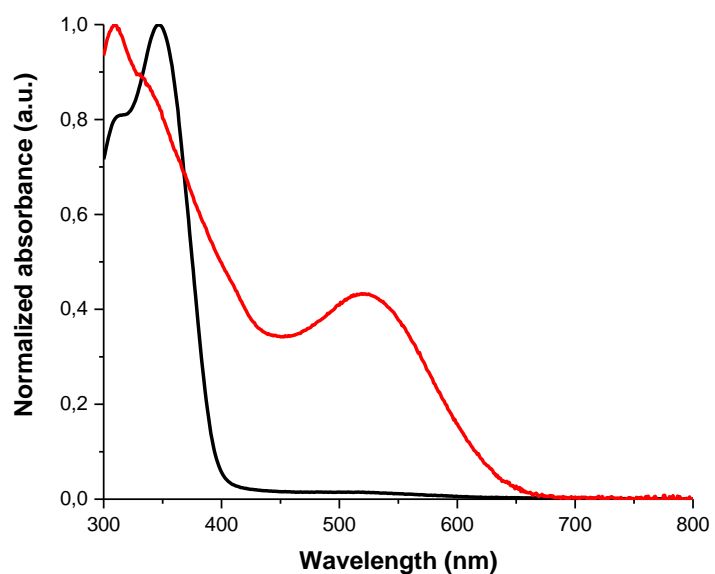
Supplementary Figure 5: Absorbance spectrum of compound NPL (toluene, 25°C, 10^{-5} M).



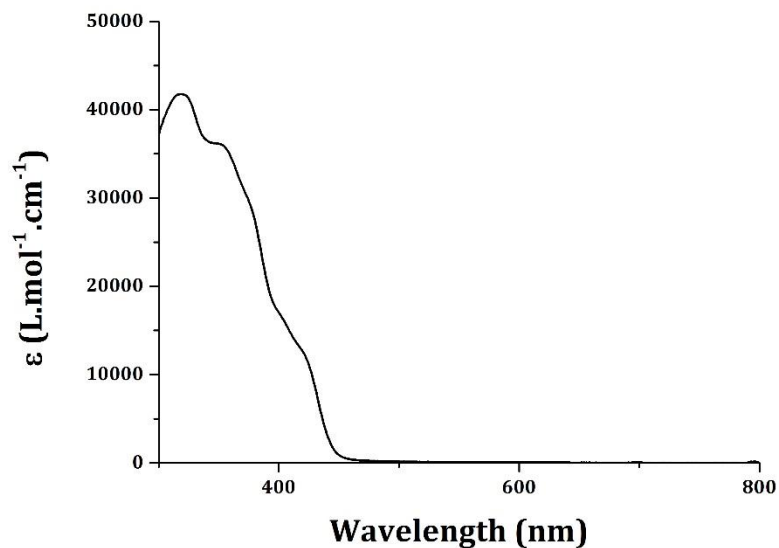
Supplementary Figure 6: Normalized absorbance spectra of compound **NPL** in the dark (black line) or under 200 W continuous polychromatic irradiation (orange line) (toluene, 25°C, 10^{-5} M).



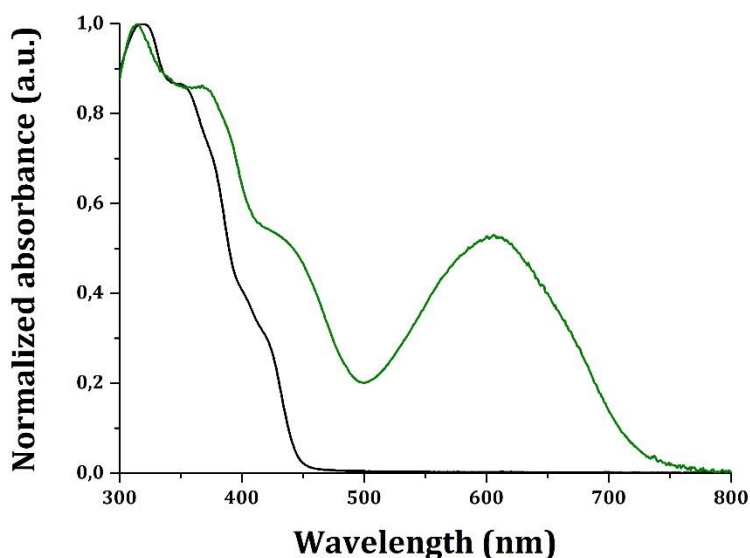
Supplementary Figure 7: Absorbance spectrum of compound **NPB** (toluene, 25°C, 10^{-5} M).



Supplementary Figure 8: Normalized absorbance spectra of compound **NPB** in the dark (black line) or under 200 W continuous polychromatic irradiation (red line) (toluene, 25°C, 10^{-5} M).



Supplementary Figure 9: Absorbance spectrum of compound **NPI** (toluene, 25°C, 10^{-5} M).



Supplementary Figure 10: Normalized absorbance spectra of compound **NPI** in the dark (black line) or under 200 W continuous polychromatic irradiation (green line) (toluene, 25°C, 10^{-5} M).

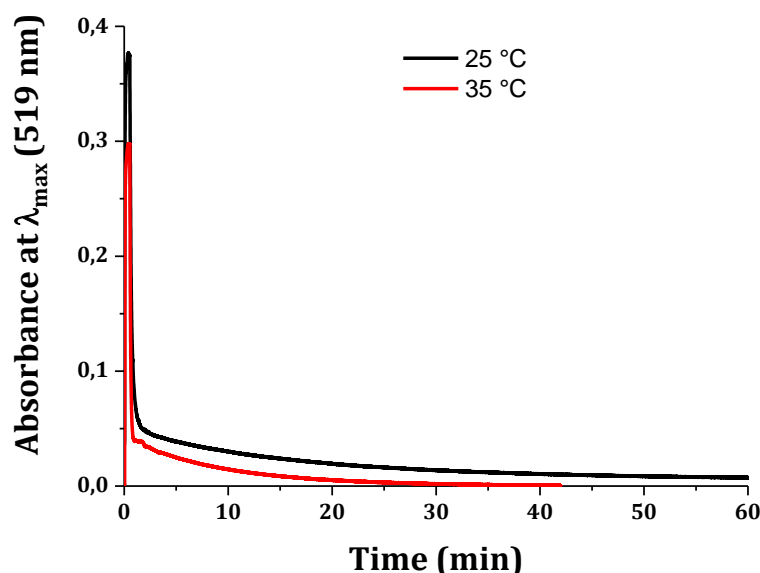
Supplementary note 4

After photo-stationary state is reached, the irradiation is switched off and the discolouration curves are registered and modelled using the following equation.

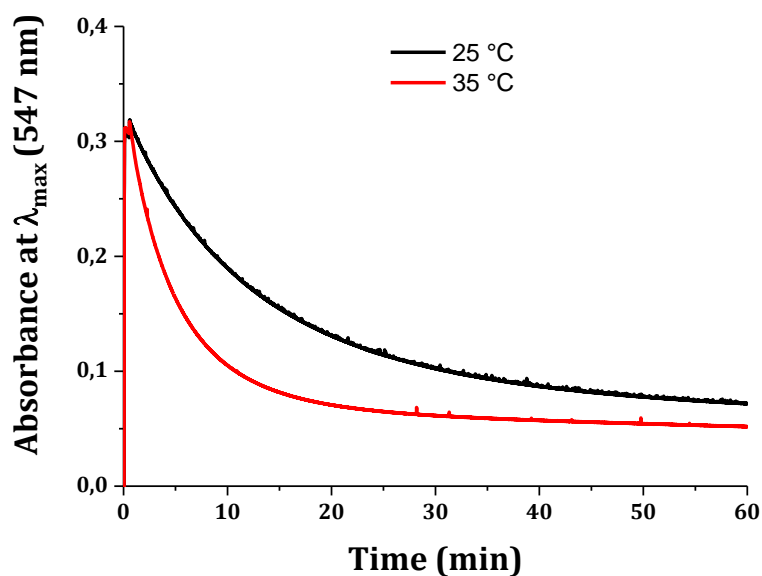
$$A(t) = a_1 e^{-k_1 t} + a_2 e^{-k_2 t} + A_\infty \quad (\text{Equation 1})$$

In this equation k_1 is the first (fast) thermal discolouration kinetic constant, a_1 the amplitude of the first kinetics, k_2 the second (slow) discolouration kinetic constant, a_2 the amplitude of the second kinetic, $A(t)$ is the absorbance as a function of time, and A_∞ the residual absorbance. The normalized discolouration curves (recorded in the dark) for **NPL**, **NPB** and **NPI** are compared in Figure 2 (Main text). It can be clearly seen that the fastest decolouration process is observed with **NPL** that shows a rapid constant k_1 of $9.8 \cdot 10^{-2} \text{ s}^{-1}$ and a slow one k_2 of $1.1 \cdot 10^{-3} \text{ s}^{-1}$. After 30 seconds, the solution recovers 80% of its transparency and the total bleaching of the solution occurs in less than 60 minutes. On the contrary, **NPB** presents the slowest discolouration process with a k_1 of $1.4 \cdot 10^{-3} \text{ s}^{-1}$ and a k_2 of $2.0 \cdot 10^{-4} \text{ s}^{-1}$. Even after several hours in the dark the solution

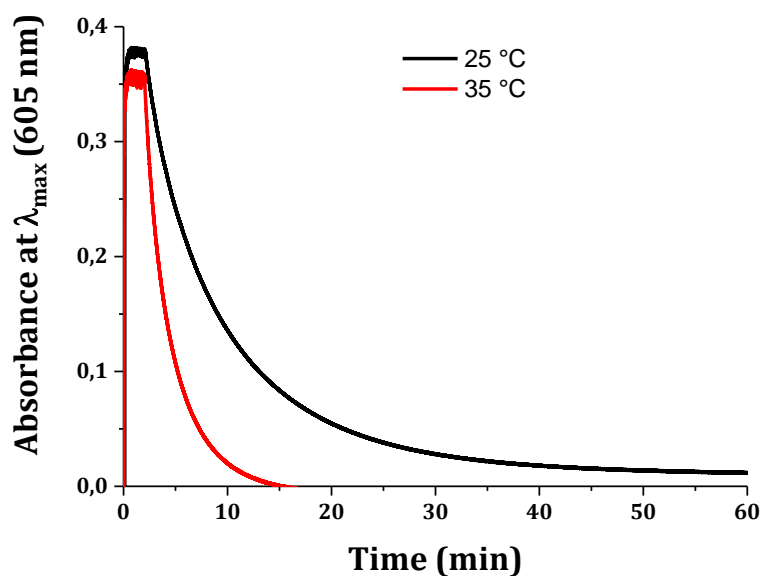
is not fully discoloured, indicating that the long-lived isomers (TT) are strongly stabilised. These results are fully consistent with previous studies showing that for unsubstituted 3,3-diphenyl-[3*H*]-naphtho[2,1-*b*]pyran a 2-orders of magnitude faster cyclo-reversion process is observed compared to the one of unsubstituted 2,2-diphenyl-[2*H*]-naphtho[1,2-*b*]pyran.⁴⁹ Interestingly, the discolouration of **NPI** can be fitted by a mono-exponential equation and the kinetic constant k_1 is relatively high, equals to $2.1 \cdot 10^{-3} \text{ s}^{-1}$ at 25°C. It takes 15 minutes for the **NPI** solution to recover 80% of its transparency and, like **NPL**, the total bleaching requires less than 60 minutes. This result confirms that the introduction of bulky substituents (*para*-phenyl-hexyl on indene) to produce steric hindrances, is an efficient way to prevent the formation of long-lived stable isomers.



Supplementary Figure 11: Absorbance of compound NPL monitored at the wavelength of maximum absorption of the opened form (519 nm), in the dark when irradiation is stopped (toluene, 10^{-5} M) at 25°C (black line) and at 35°C (red line).



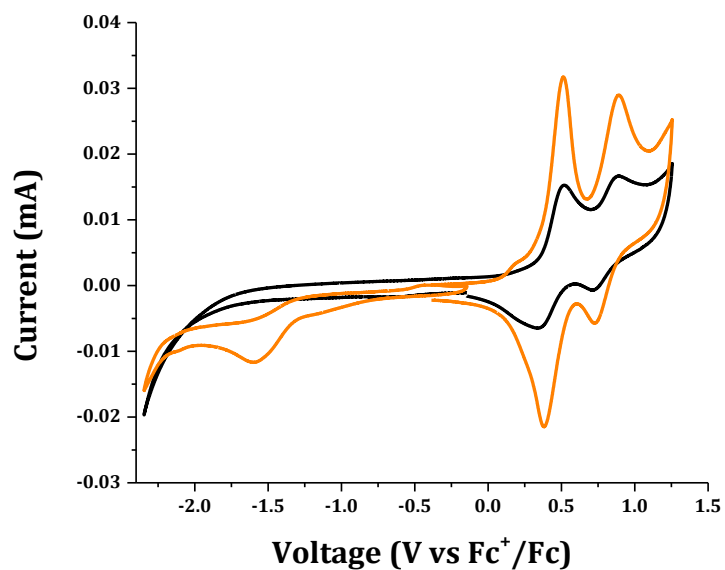
Supplementary Figure 12: Absorbance of compound **NPB** monitored at the wavelength of maximum absorption of the opened form (547 nm), in the dark when irradiation is stopped (toluene, 10^{-5} M) at 25°C (black line) and at 35°C (red line).



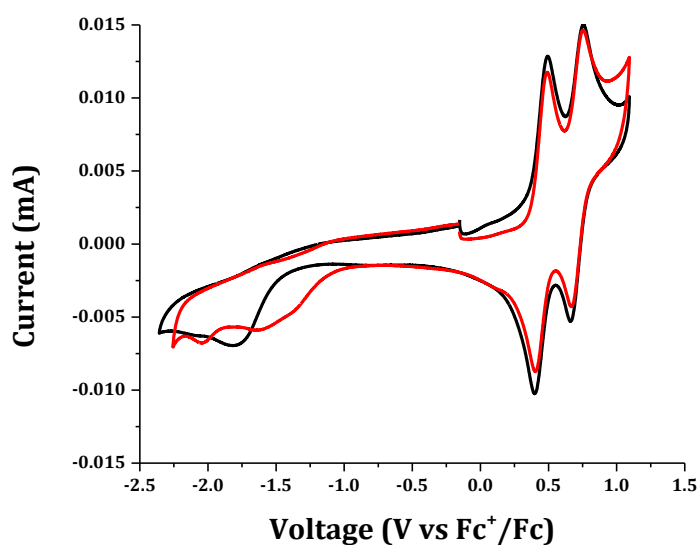
Supplementary Figure 13: Absorbance monitored at the wavelength of maximum absorption of the opened form (605 nm), in the dark when irradiation is stopped (toluene, 10^{-5} M) at 25°C (black line) and at 35°C (red line).

Supplementary note 5

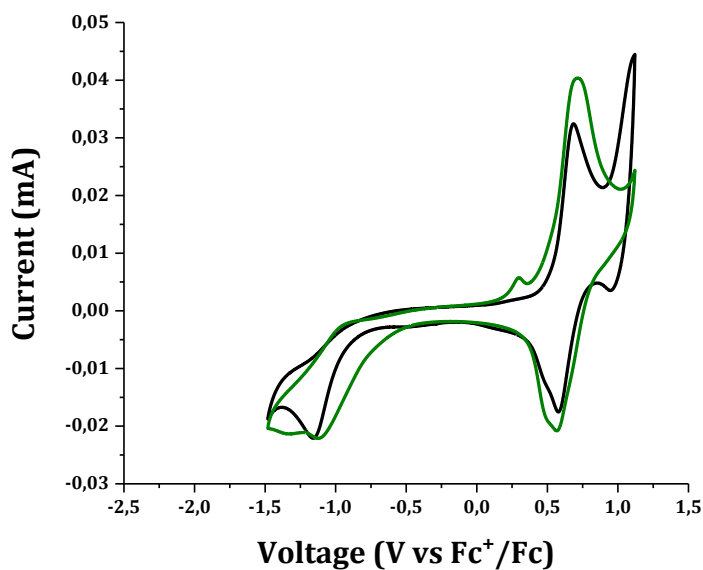
For application in DSSCs, it is crucial to verify that the dyes possess energy levels correctly positioned with respect to the conducting band of the oxide (for the LUMO) and with respect to the redox potential of the redox couple in the electrolyte (for the HOMO). With the goal to follow the variation in the optoelectronic properties swapping from the closed to the open form, the energy levels of the frontiers orbitals were evaluated by cyclic voltammetry (CV) in dichloromethane with ferrocene as the internal reference before and after irradiation. (see Methods for experimental details). The cyclic voltammetry traces are reported in **Supplementary Figures 14, 15 and 16** for NPL, NPB and NPI respectively. When positive potentials are applied, the dyes exhibit two reversible oxidation waves corresponding to two oxidation/re-reduction processes. Upon application of negative potentials, the dyes undergo a non-reversible reduction process.



Supplementary Figure 14: cyclic voltammetry trace of compound NPL (DCM, 25°C) under dark (black line) and after irradiation (orange line).



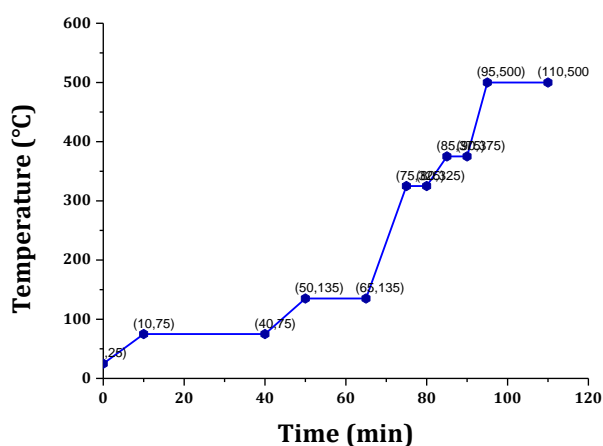
Supplementary Figure 15: cyclic voltammetry trace of compound NPB (DCM, 25°C) under dark (black line) and after irradiation (red line).



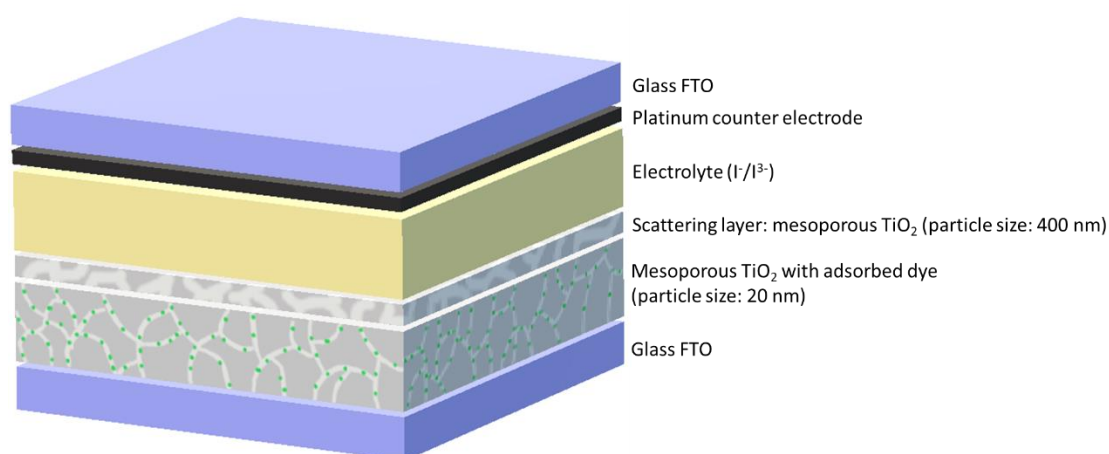
Supplementary Figure 16: cyclic voltammetry trace of compound NPI (DCM, 25°C) under dark (orange line) and after irradiation (green line).

Supplementary Note 6

The use of a commercial electrolyte *i.e.* Iodolyte whose composition is made up of 0.5 M 1-butyl-3-methyl-imidazolium iodide (BMII), 0.1 M lithium iodide, 0.05 M iodine and 0.5 M *tert*-butyl-pyridine (tBP) in acetonitrile led to poor performances with low J_{sc} . We report the results of the optimisation of the NPI-based solar cells in **Supplementary Tables 11 to 13** and in **Supplementary Figures 19 to 21**.



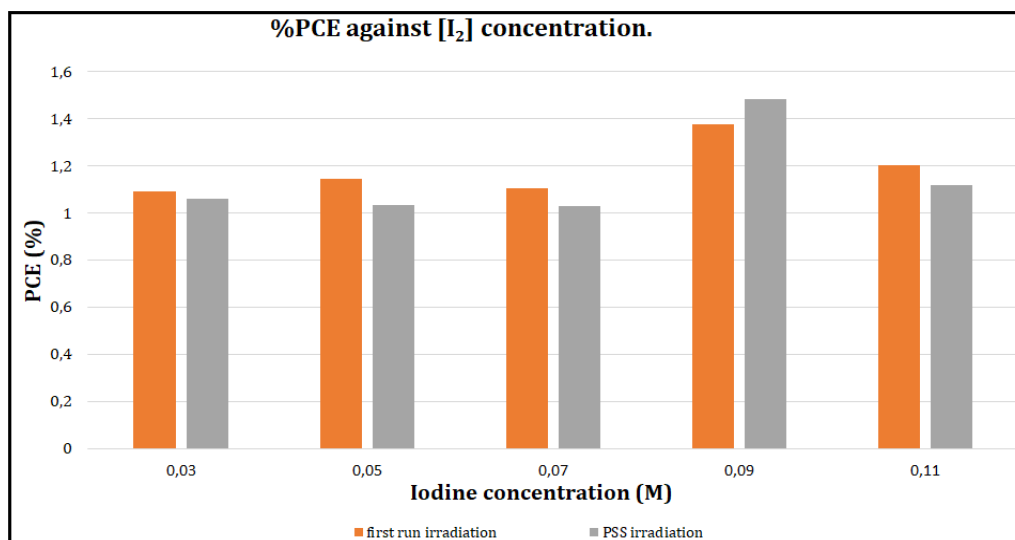
Supplementary Figure 17: Temperature evolution for the electrodes thermal annealing process.



Supplementary Figure 18: Schematic device structure of the dye solar cells

Iodine concentration (M)	J_{sc} (mA.cm⁻²)	V_{oc} (V)	FF (%)	PCE (%)
0.03	2.68	0.56	72	1.08
0.05	2.82	0.57	73	1.17
0.07	2.91	0.58	72	1.21
0.09	3.23	0.62	75	1.48
0.11	2.89	0.57	69	1.13

Supplementary Table 11. Effect of increasing iodine concentration on J_{sc} , V_{oc} , and FF for NPI-based opaque solar cells.



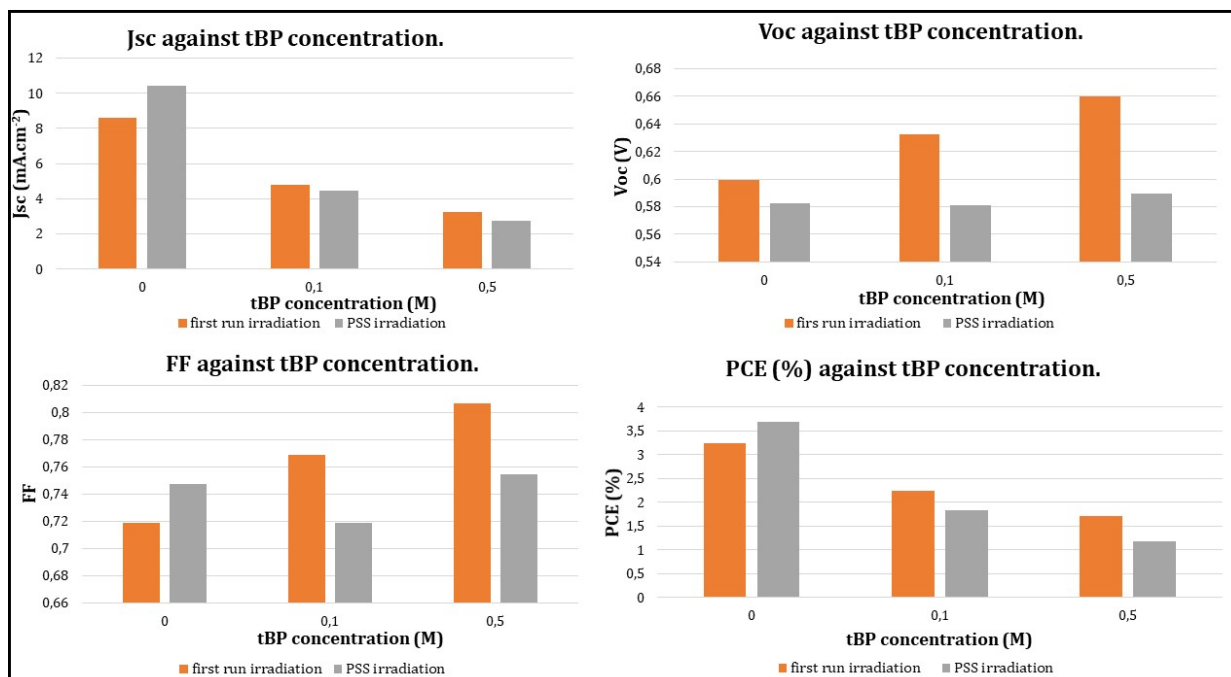
Supplementary Figure 19: Effect of increasing iodine concentration on PCE for NPI-based opaque cells.

tBP concentration (M)	J_{sc} (mA.cm ⁻²)	V_{oc} (V)	FF (%)	PCE (%)
0	8.62	0.59	71	3.25
0.1	4.79	0.63	76	2.23
0.5	3.26	0.66	80	1.72

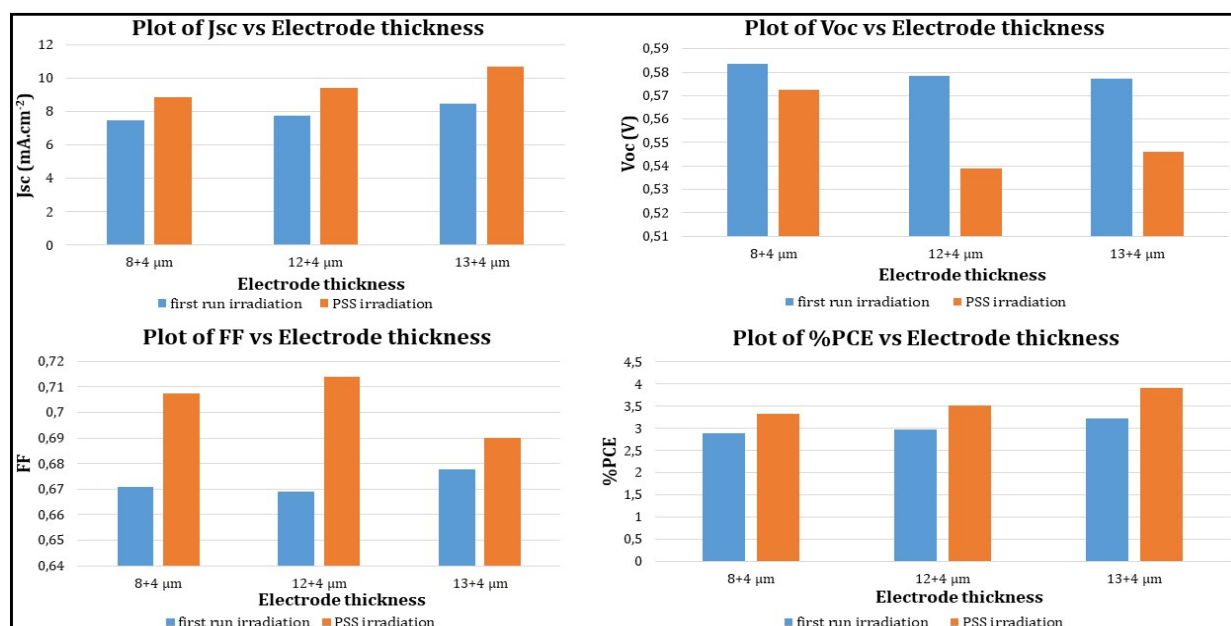
Supplementary Table 12. Effect of increasing tBP concentration on key electrical parameters (J_{sc} , V_{oc} , and FF and PCE) after first run irradiation for NPI-based opaque solar cells.

tBP concentration (M)	J_{sc} (mA.cm ⁻²)	V_{oc} (V)	FF (%)	PCE (%)
0	10.44	0.58	74	3.69
0.1	4.45	0.58	71	1.82
0.5	2.76	0.58	75	1.17

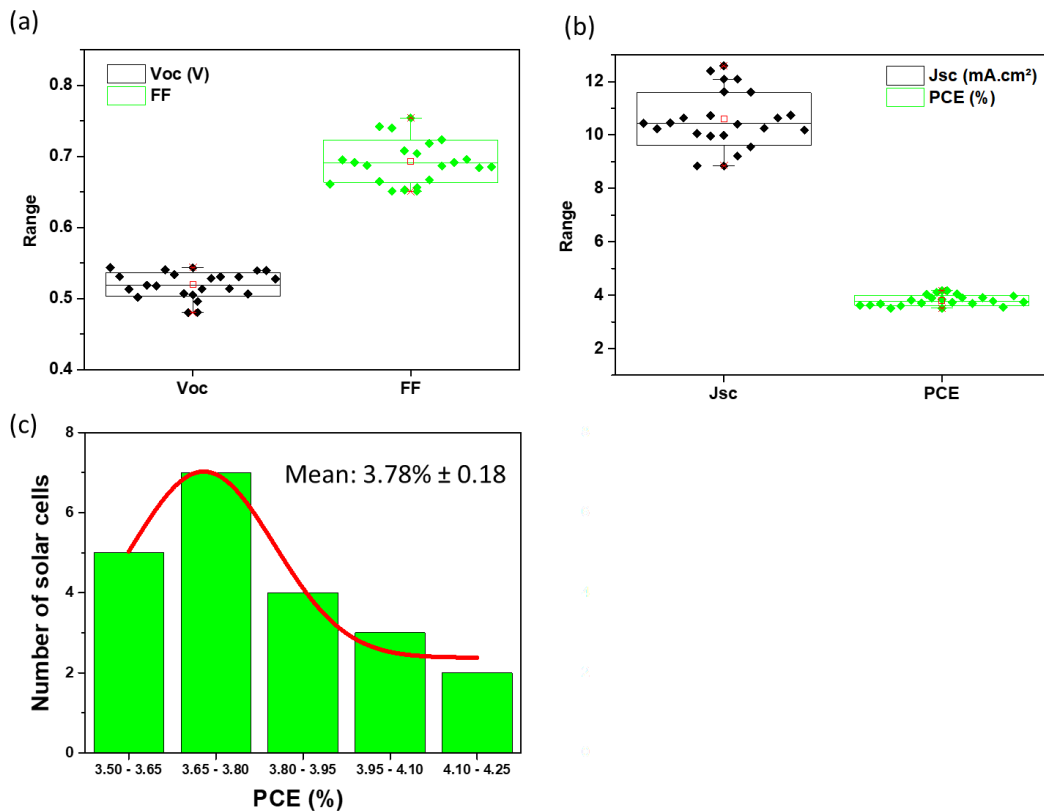
Supporting Table 13. Effect of increasing tBP concentration on key electrical parameters (J_{sc} , V_{oc} , and FF and PCE) at PSS for NPI-based opaque solar cells.



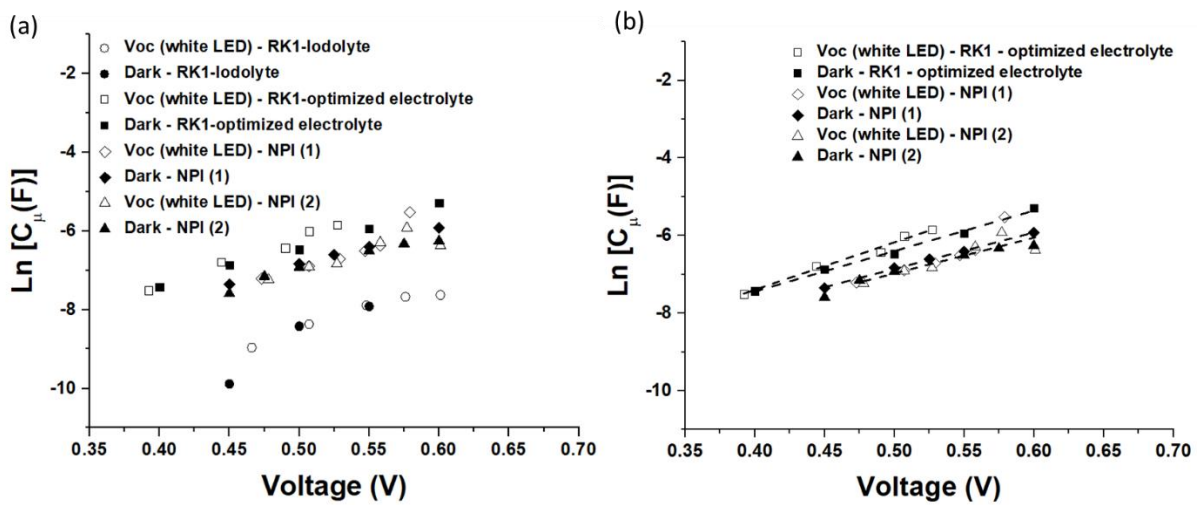
Supplementary Figure 20: Effect of increasing tBP concentration on J_{sc} , V_{oc} , FF, and PCE for NPI-based opaque cells.



Supplementary Figure 21: Effect of electrode thickness on J_{sc} , V_{oc} , FF, and PCE for NPI-based opaque cells.



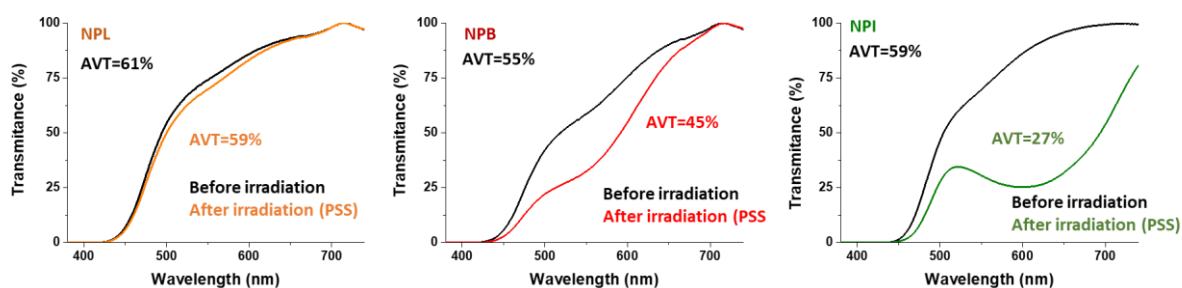
Supplementary Figure 22: Statistical data for V_{oc} and FF (a), J_{sc} and PCE (b), and performance reproducibility (c) over 21 NPI-based opaque solar cells.



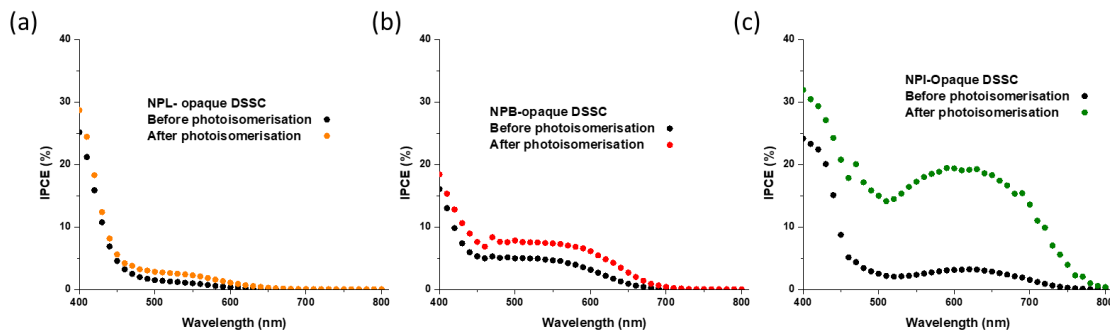
Supplementary Figure 23. a) Chemical capacitance data as a function of DC voltage for NPI-based, and RK1 reference solar cells. Values extracted from fittings of the recombination arc in the EIS data to a single RC element. a) Dashed lines are fits to Eq. (3) in the main text.

Cell type	R_{ct} (dark)	R_{ct} (red)	R_{ct} (blue)	R_{ct} (white)	C_{μ} (dark)	C_{μ} (red)	C_{μ} (blue)	C_{μ} (white)
RK1-Iodolyte	0.70			0.74	0.55			0.17
RK1-Optimized	0.48			0.69	0.27			0.32
NPI-1	0.73			1.24	0.24			0.25
NPI-2	0.71	0.87	1.02	1.12	0.19	0.31	0.33	0.23

Supplementary Table 14. α and β parameters obtained from fittings to Equations (2) and (3)⁴⁹ of the main text for RK1-reference cells and NPI-based solar cells.



Supplementary Figure 24: Variation of the Average Visible Transmittance of semi-transparent photochromic solar cells before irradiation and after light soaking (PSS reached under standard irradiation conditions).



Supplementary Figure 25: IPCE spectra of opaque solar cells before and after light soaking (a) with NPL, (b) with NPB, (c) with NPI.

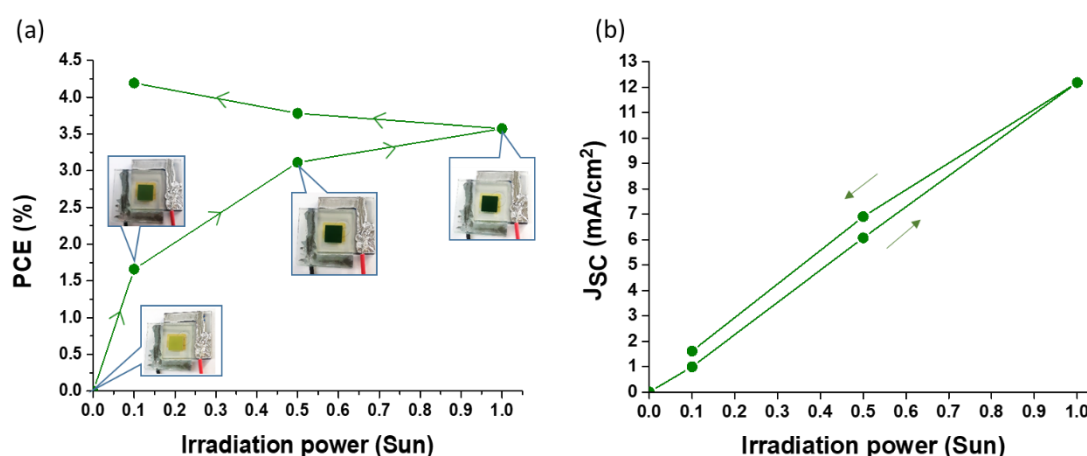
Supplementary Note 7

The PCE of the photochromic solar cells is expected not to be the same going from low light irradiation to 1 Sun and from 1Sun to low light irradiation because of the activation of the dye. To demonstrate that, we have fabricated **NPI**-based opaque solar cells and investigated their photovoltaic performances and J_{sc} as the function of the light intensity. This experiment was carried out from 0.1 Sun to 1 Sun and after the complete coloration of the solar cell we performed the measurements from 1 Sun to 0.1 Sun.

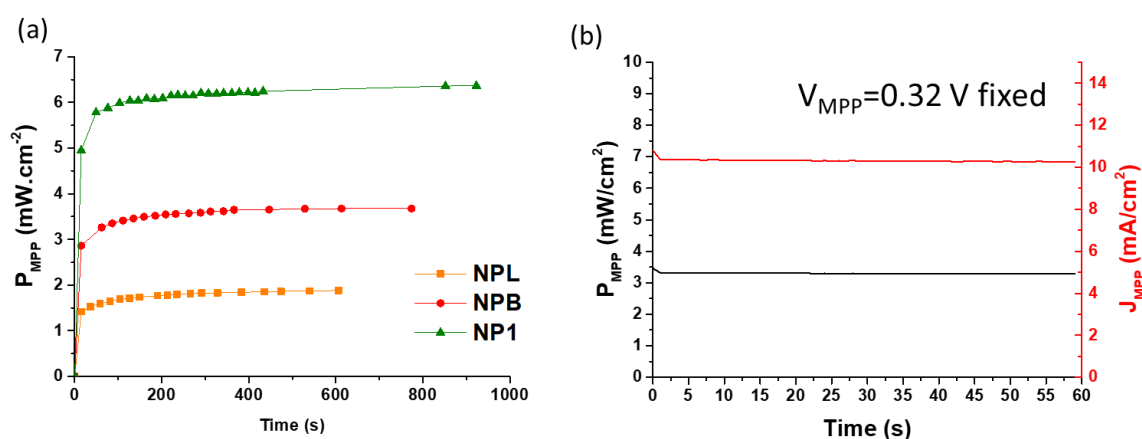
On the following **Supplementary Figure 26**, we report the PCE and the J_{sc} of the solar cells exposed to 0.1 Sun, 0.5 Sun and 1 Sun with increasing and decreasing light intensity. Interestingly, the PCE is increasing constantly even at low light-irradiation after activation of

the solar cell at 1 Sun. This can be explained by the presence of more dyes in the opened form on the electrode. Consequently, when increasing the light intensity, the J_{sc} at 0.5 Sun is 6.07 mA/cm^2 and when decreasing the light intensity the J_{sc} at 0.5 Sun is 6.90 mA/cm^2 .

This experiment further confirms that the solar cells adapt their colour and J_{sc} as a function of the power of irradiation and we demonstrate that they can be more efficient under low-light power after activation of the dyes.



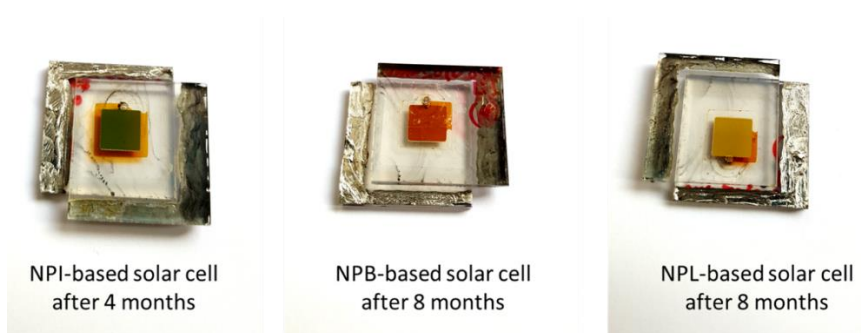
Supplementary Figure 26: Evolution of the (a) PCE and colour, and (b) J_{sc} of NPI-based opaque solar cells with increasing and decreasing light intensity (from 0.1 Sun to 1 Sun and the reverse)



Supplementary Figure 27: (a) Evolution of the maximum power of NPL, NPB and NPI-based solar cells (fabricated using optimized conditions) at the maximum power point (MPP) under continuous irradiation (simulated AM1.5G 1 sun illumination). (b) steady-state output of the best cell (NPI-based opaque cell).

Supplementary Note 8

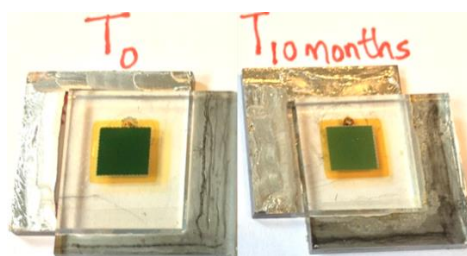
In order to shed light on the source of the degradation we have studied solar cells few months after their fabrication. The pictures below clearly demonstrate that some of the devices are degraded because of the leak or the evaporation of the electrolyte.



Supplementary Figure 28: Picture of NPI, NPB, NPL-based solar cells after several month of storage showing the leakage or evaporation of the electrolyte.

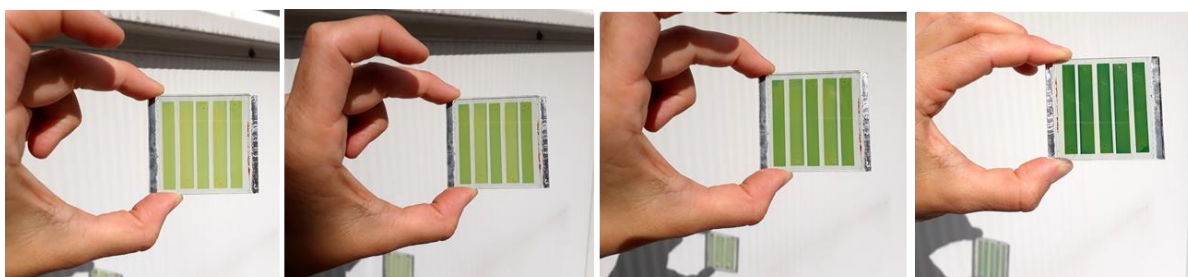
We also have compared the colourability at the photostationary state of NPI-based solar cells freshly prepared and after 10 months of storage. It appears clearly that the photoanode is less coloured after ageing. The solar cells show a maximum PCE of 0.7% that is not improved even refilling the cells with a fresh electrolyte.

The loss of colourability is not attributed to desorption of the dye because the electrolyte does not show any photochromic behaviour and remains yellow under illumination. This indicates that the degradation is not related to desorption of the dye but probably to the degradation of the dye itself. Previous studies have demonstrated that naphthopyrans can undergo several degradation pathways under prolonged irradiation in solvents.⁴⁹

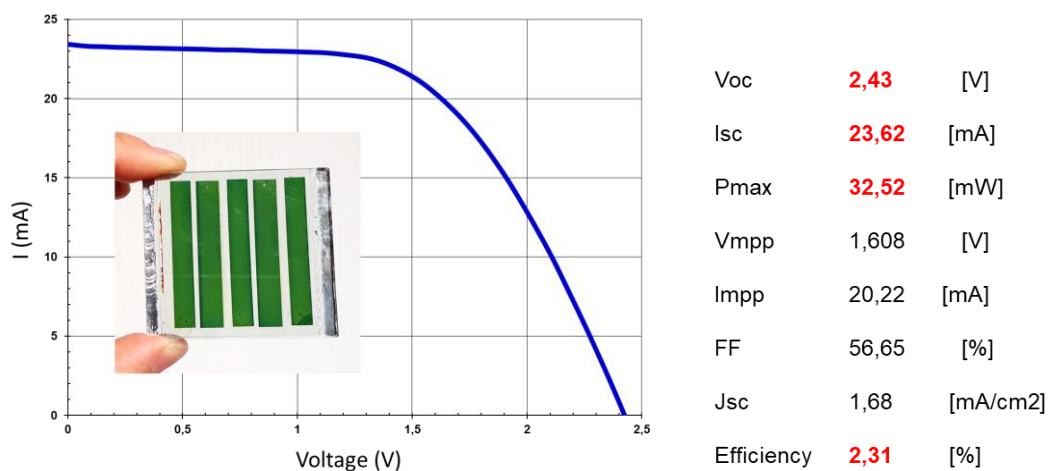


Supplementary Figure 29: Pictures of NPI-based opaque solar cells in the photo-stationary state, freshly prepared (left) and 10 months after the fabrication (right).

a)



b)



Supplementary Figure 30: a) Pictures of a photo-chromo-voltaic mini-module (active area 14.08 cm²) after different times of exposure to ambient light at 20°C. b) $I(V)$ curve of a mini-module and photovoltaic parameters obtained at the photo-stationary state, under standard illumination AM 1.5G 1000W/m², 25°C.